Journal of Advanced Research xxx (xxxx) xxx

Contents lists available at ScienceDirect

Journal of Advanced Research

journal homepage: www.elsevier.com/locate/jare

# Genome-wide characterization and adaptive evolution of favorable *gibberellin 2-oxidase* alleles contributing to wheat agronomic traits

Yingjie Bian [a,b,1], Jiayu Dong [c,1], Lingli Li [a,1], Dengan Xu [d,1], Xiuling Tian [a], Yan Dong [e], Jianqi Zeng [a], Qiang Cao [a], Yachao Dong [a], Lina Xie [a], Bingyan Liu [a], Kejia Qu [a], Yuheng Chao [a], Rui Che [a], Jindong Liu [a], Yong Zhang [a], Xianchun Xia [a], Daojie Sun [b,*], Fei Lu [a,*], Zhonghu He [a,*], Shuanghe Cao [a,*]

[a] *State Key Laboratory of Crop Gene Resources and Breeding/National Wheat Improvement Center, Institute of Crop Sciences, Chinese Academy of Agricultural Sciences, Beijing 100081, China*
[b] *College of Agronomy, Northwest A&F University, Yangling 712100 Shaanxi, China*
[c] *State Key Laboratory of Plant Cell and Chromosome Engineering, Institute of Genetics and Developmental Biology, Innovative Academy of Seed Design, Chinese Academy of Sciences, Beijing 100101, China*
[d] *College of Agronomy, Qingdao Agricultural University, Qingdao 266109, China*
[e] *Crop Research Institute, Ningxia Academy of Agricultural and Forestry Sciences, 490 Huanghe Road, Yinchuan 750002 Ningxia, China*

## HIGHLIGHTS

- *Gibberellin 2-oxidase* (*GA2ox*) genes are key regulators of agronomic traits in crops.
- Two wheat *GA2ox* family members were previously validated as causal genes of reduced height (*Rht*) loci.
- Eight new favorable haplotypes of wheat *GA2ox* genes reduce plant height without yield penalty.
- The adaptive evolution and application prospects of these favorable haplotypes were evaluated.

## GRAPHICAL ABSTRACT

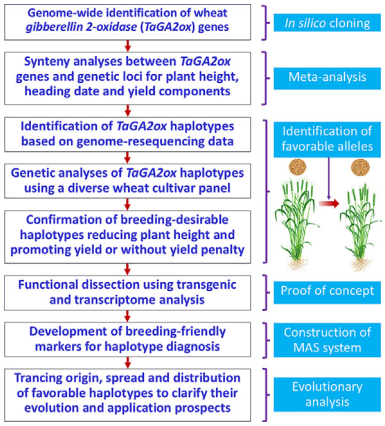


## ARTICLE INFO

*Article history:*
Received 16 December 2024
Revised 2 August 2025
Accepted 16 August 2025
Available online xxxx

*Keywords:*
Agronomic traits
Evolution
Favorable variation
*TaGA2ox*
*Triticum aestivum*

## ABSTRACT

*Introduction:* Gibberellins are essential phytohormones that regulate plant growth and development. Gibberellin 2-oxidases (GA2oxs) deactivate bioactive gibberellin isoforms and many *GA2ox* genes have been validated as key regulators of agronomic traits in model plants and crops. However, there are few studies on *GA2ox* genes in wheat, one of the most important staple crops.
*Objective:* This study aims to identify favorable alleles of wheat *GA2ox* genes (*TaGA2oxs*) and assess their application in wheat improvement.
*Methods:* We developed an efficient pipeline that integrates population genomics, transgene, transcriptome and evolutionary analyses to systemically dissect genetic effects of *TaGA2ox* variations on agronomic traits.
*Results:* We identified 40 *TaGA2oxs* by genome-wide *in silico* cloning, defined 25 C19-type and 15 C20-type members based on sequence similarity and specified *TaGA2ox* family expansion by genomic

* Corresponding authors.
*E-mail addresses:* Sunwheat@nwafu.edu.cn (D. Sun), flu@genetics.ac.cn (F. Lu), hezhonghu02@caas.cn (Z. He), caoshuanghe@caas.cn (S. Cao).
[1] These authors contributed equally to this work.

https://doi.org/10.1016/j.jare.2025.08.025


Please cite this article as: Y. Bian, J. Dong, L. Li et al., Genome-wide characterization and adaptive evolution of favorable *gibberellin 2-oxidase* alleles contributing to wheat agronomic traits, Journal of Advanced Research, https://doi.org/10.1016/j.jare.2025.08.025

polyploidization, duplication and translocation events. Functional *TaGA2oxs* were predicted by spatiotemporal expression assays, genetic *meta*-analysis and genome microsynteny-based phylogeny. We retrieved 52 major haplotypes at 19 *TaGA2ox* loci based on genome resequencing data for representative wheat cultivars and developed diagnostic molecular markers. In addition to previously-validated favorable haplotypes *Rht12b* and *Rht24b* that reduce plant height and have no yield penalty, eight new favorable haplotypes of *TaGA2oxs* were identified by marker-trait association analysis. Among them, *TaGA2ox8-B1-1_hap1*, *TaGA2ox8-B1-2_hap1* and *TaGA2ox8-B1-3_hap1* formed a tandem duplicate gene cluster associated with reduced plant height and increased grain yield. *TaGA2ox8-B1-2* as proof of concept was functionally validated to modulate major agronomic traits by transgene assays; its downstream genes and effect on gibberellin homeostasis were also identified by transcriptome, enzyme activity and hormone quantitative analyses. We further traced the origin, spread and distribution of favorable haplotypes to clarify their evolutionary history and application prospects.

*Conclusion:* These findings not only provide valuable genetic resources and molecular tools for wheat improvement but also broaden genetic insight into gibberellin-mediated wheat morphogenesis, acclimation and yield formation.



## Introduction

Gibberellin (GA) is an important phytohormone regulating multiple growth and developmental processes, including stem and root elongation, floral induction, grain development and seed germination [1,2]. Accordingly, GA modulates agronomic traits in crops through its biosynthesis, catabolism and signal transduction. DELLA is a core factor in the GA signal transduction pathway and has been specified functionally [3,4]. Wheat (*Triticum aestivum* L.) Green Revolution (GR) genes *Rht-B1b* and *Rht-D1b* encode truncated DELLA proteins [5,6]. GA biosynthesis and catabolism are also crucial for plant growth and development. Three classes of enzymes GA 20-oxidase (GA20ox), GA 3-oxidase (GA3ox) and GA 2-oxidase (GA2ox) play key roles in maintaining GA homeostasis [7]. GA20ox is a rate-limiting enzyme that catalyzes a series of intermediate steps in GA production. The *GR* gene *semi-dwarf 1* (*sd1*) in rice is a loss-of-function allele of *OsGA20ox2* that reduces lodging and increases yield [8]. GA3ox catalyzes the final step in production of bioactive GA [9]. By contrast, GA2ox catalyzes the deactivation of bioactive GA isoforms or their precursors through a 2$\beta$-hydroxylation reaction. *GA2ox* genes are divided into C19-clade and C20-clade subfamilies according to the catalytic substrates [10]. Enhanced expression of *C19-GA2ox* genes usually causes vegetative and reproductive abnormalities, such as severe dwarfing and sterility, whereas C20-GA2ox overproduction moderately decreases bioactive GA levels, generally resulting in appropriate dwarfing phenotypes with improved yield potential [11–13]. Wheat has lagged far behind model species, such as rice and Arabidopsis, in genome assembly due to a large (~16 Gb), hexaploid and complex genome that contains more than 85 % repetitive sequences [14]. Low-efficiency transformation technology in wheat hinders functional research ten years ago [15]. The advent of high-quality genomic assembly, high-throughput genotyping and high-efficiency transgene technologies and resultant databases permits comprehensive characterization of the variations of the wheat *GA2ox* genes (*TaGA2oxs*) and systemic dissection of their genetic effects on agronomic traits. A few genetic studies of *TaGA2oxs* have also been conducted. The widely-used favorable *reduced height* (*Rht*) genes, *Rht12b* and *Rht24b*, encode TaGA2oxA13 and TaGA2oxA9, respectively, and have no adverse effect on yield in wheat [16–18]. In all, *GA2oxs* are an important gene family modulating plant stature and yield potential. However, the effects of most *TaGA2oxs* on agronomic traits are largely unknown.

During recent years, reference genome assembles of many wheat accessions were released, including Chinese Spring, Zang 1817, Fielder, Kenong 9204, Aikang 58 and more than 10 elite wheat cultivars from the 10 + Genome Project [14,19–23]. Release of the wheat reference genome and decreasing costs of high-throughput resequencing allow researchers to investigate genomic variations across hundreds of accessions [19,24–27]. Additionally, genome-resequencing information is organized and integrated into the SnpHub with a portal to retrieve allelic variations of target genes (https://wheat.cau.edu.cn/Wheat_SnpHub_Portal) [28]. Here, we performed a comprehensive identification of *TaGA2oxs* by a genome-wide homology search. The allelic variations of *TaGA2oxs* were retrieved from the genome-resequencing databases and their haplotypes (a group of variation sites inherited together) were also defined. We further analyzed the genetic effects of major haplotypes on agronomic traits and accordingly determined favorable variations. A *TaGA2ox* was exemplified as a representative to validate function in modulating GA homeostasis and agronomic traits by transgene, hormone quantification and transcriptome assays. We also traced the origin and spread of desirable haplotypes and uncovered their sequential dynamic distribution in Chinese core wheat germplasms. These outcomes provide breeding selection signatures and molecular tools for wheat improvement, and an efficient procedure that integrates population genomics, transgene assays and evolutionary analysis to genome-wide identify favorable alleles of genes of interest.

## Materials and methods

### *Plant materials and growth conditions*

A natural population including 166 elite wheat cultivars from the Huang-Huai River region, the largest wheat growing area in China, was used to analyze the genetic effects of *TaGA2ox* haplotypes. The soil types of planting sites in the Huang-Huai River region are brown or sandy ginger black soils. Wheat was irrigated once at each of the three stages, pre-overwintering, stem elongation and grain filling. The agronomic traits of this population, including plant height, heading date, yield components (spike number per $m^2$, grain number per spike, and thousand grain weight), and grain yield, were investigated in six environments reported by previous study [29].

Transgenic recipient Fielder and overexpression lines were grown at Shijiazhuang in Hebei province. The Fielder and transgenic lines were planted in 2 m eight-row plots and 0.3-m row spacing, with 60 seeds per row. The randomized complete blocks design with three replications was employed. Field management was performed according to local practice. Plant height was measured from the ground to spikes (awns excluded) at grain fill stage (Feekes 11.4). Heading date was recorded at complete emergence of spikes and represented as days from sowing to heading (Feekes

10.5). Spike number per plant (SN) was estimated by counting spikes after harvest. For grain number per spike (GNS), thousand grain weight (TGW), grain length and grain width, 20 randomly selected spikes were harvested in each plot with three replications, and these traits were measured using the SC-G Seed detector (WSeen Co. Ltd, Hangzhou).

*Identification of TaGA2ox members in wheat*

Eleven OsGA2ox members were reported in a previous study (Table S1) [30]. OsGA2ox protein sequences were retrieved from the China Rice Data Center (https://www.ricedata.cn/gene/) and RGAP 7 (https://rice.uga.edu/) database and used as queries to search the International Wheat Genome Sequencing Consortium (IWGSC) RefSeq v1.1 protein database using Blastp (https://plants.ensembl.org/Triticum_aestivum/Tools/Blast?db=core). Putative TaGA2ox proteins were identified with an E-value threshold of 1e-5 [31–33]. Then, unique TaGA2oxs were used for further analysis by removing redundant sequences. The Pfam (version 37.3) (https://pfam.xfam.org) database was employed to verify wheat GA2oxs with DIOX_N (PF14226) and 2OG-FeII_Oxy (PF03171) domains. The same method had also been applied to identify GA2oxs in genomes from different wheat varieties.Physical positions of *TaGA2oxs* in chromosomes were identified according to the IWGSC RefSeq v1.1, and their distribution in chromosomes were visualized using MapChart v2.3 [34].

*Phylogenetic and synteny analysis of GA2oxs*

GA2oxs in maize, *Brachypodium distachyon* and barley were retrieved from EnsemblPlants version 56 (https://plants.ensembl.org/index.html; Table S1). Sequences of GA2oxs in Arabidopsis were downloaded from TAIR (https://www.arabidopsis.org). Multiple alignment of GA2ox sequences was performed using the ClustalW program with default parameters. A phylogenetic tree was constructed by the NJ (neighbor-joining) method with 1000 bootstrap repetitions in MEGA 7.0 [35]. GA2ox members in wheat were numbered according to their orthologous relationships with OsGA2ox members and were named following the updated guideline of gene nomenclature [36]. We identified orthologous *GA2ox* genes across species by genome collinearity. The collinearity program in the Triticeae-GeneTribe (https://wheat.cau.edu.cn/TGT/index.html) with setting number of neighboring genes at 10 was employed to perform regional synteny analysis [37]. GeneTribe refers to the similarity of a gene pair using the BLAST score ratio method [38]. The criteria defining the duplicated-gene events are that the length of the alignment sequence covers at least 80 % of the longest gene and the similarity of the aligned regions exceeds 70 % [39].

*In silico expression analysis*

Transcriptomic data used to analyze the expression patterns of *TaGA2oxs* in different tissues and growth stages of Chinese Spring were downloaded from the WheatOmics 1.0 database (https://202.194.139.32/expression/wheat.html) [40]. In this database, the division of growth stages adopted the Zadoks scale for wheat [41]. Uniformed corrective $\log_2$(TPM + 1) (TPM, transcripts per million) values of each *TaGA2ox* in different tissues and stages were displayed on a heatmap using using TBtools-II v2.152 [42].

*Co-localization analysis of TaGA2oxs and quantitative trait loci (QTL) for agronomic traits*

Genetic loci for plant height and yield component traits from linkage mapping and association analysis were summarized previously [43,44]. We also collected information of genetic loci for heading date [45–51]. Physical locations of genetic loci were delimited by the closest linked markers or genetic intervals according to the IWGSC RefSeq1.0 (https://plants.ensembl.org/index.html) [14]. The genes of interest are defined as overlapping with QTL for agronomic traits if they are co-localized in the physical interval of less than 10 Mb following previous reports [43,44]. QTL overlapping or adjacent to *TaGA2oxs* were shown by MapChart v2.3 [34].

*Polymorphic site calling based on genome resequencing data*

Genome resequencing information of 137 wheat cultivars was used to identify allelic variations of *TaGA2oxs* (https://wheat.cau.edu.cn/WheatUnion/; Table S2) [19,25]. Sequence variations in genomic regions spanning 1.5-kb upstream and 500-bp downstream of open reading frames (ORFs) were retrieved and analyzed. To identify causal, their variations causing missense mutation, premature stop, frameshift or splicing mutations in ORFs, and upstream promoter region and polyadenylation signal sites were used to define haplotypes.

*Marker development and genotyping assays*

The function 'Design & Check' in WheatOmics 1.0 (https://202.194.139.32/PrimerServer) [40] was used to design gene-specific primers with 60–65 °C annealing temperature for sequence-tagged site (STS) and target sequencing (GBTS) markers. PCR was performed in 20 μl reaction volumes containing 10 μl of Taq 2 × PCR Mix plus Dye (Cat#RK20608, ABclonal, Wuhan), 1 μl of each primer (10 μmol/L) and 150 ng of genomic DNA using an ABI Thermal Cycler (Gene Co., Ltd, Shanghai). PCR programs include three steps: an initial denaturation at 95 °C for 5 min, 37 amplification cycles of 40 s at 95 °C, 40 s at 60 °C and 30–60 s at 72 °C, and a final extension at 72 °C for 5 min. The resultant DNA fragments of STS markers were separated in 1.5 % agarose gels to detect polymorphisms in fragment length. For GBTS markers, the amplified products were sequenced at the Sangon Biotech Institute (https://www.sangon.com/) using specific sequencing primers (Table S3).

The flanking sequences of polymorphic sites were obtained from WheatOmics 1.0 (https://202.194.139.32/getfasta/index.html) [40] and submitted to PolyMarker (https://www.polymarker.info/) to design the primers of kompetitive allele-specific PCR (KASP) markers. Allele-specific primers were tailed with the sequences 5′-GAAGGTGACCAAGTTCATGCT-3′ or 5′-GAAGGTCG GAGTCAACGGATT-3′, complementary to FAM-labeled and HEX-labeled probes, respectively. Primer mixtures contained 12 μl of each allele-specific primer (100 μmol/L), 30 μl of common primer (100 μmol/L), and 46 μl of dd$H_2O$. KASP assays were performed in 3 μl mixtures including 100 ng of dried genomic DNA, 1.5 μl of 2 × KASP master mix (Cat#AQP-002L, JasonGen, Beijing), 1.5 μl of double-distilled $H_2O$ and 0.0336 μl of KASP primer mixture. PCR was conducted as follows: initial denaturation at 94 °C for 10 min, and 10 cycles of 94 °C for 20 s and touchdown at 65 °C decreasing by 0.8 °C per cycle for 60 s, followed by 40 cycles of 94 °C for 20 s, and 57 °C for 60 s. Fluorescence of samples was detected on a PHERAstarplus (BMG Labtech GmbH, Ortenberg, Germany) and analyzed using KlusterCaller v4.1.1.24078 (LGC, Hoddesdon, UK).

*Vector construction and genetic transformation*

The full-length coding sequence (CDS) of *TaGA2ox8-B1-2* from wheat cultivar Chinese Spring (*TaGA2ox8-B1-2_hap1*) was cloned into the wheat overexpression vector pUbiTCK303 with maize ubiquitin promoter [52]. The resultant construct was transformed

into *Agrobacterium tumefaciens* strain EHA105 by the chemical transformation method (https://www.weidibio.com/display.php?id = 302) [53]. Genetic transformation was implemented by infecting immature embryos of wheat cultivar Fielder with strain EHA105 carrying the given construct [54]. Primers for identifying transgene-positive lines are listed in Table S3.

*Enzyme activity assays and quantitative analysis of GA isoforms*

Stems at jointing stage (Feekes 7.0) were promptly frozen in liquid nitrogen and used to measure GA2ox activity with a Plant GA2oxidases ELISA KIT following the manufacturer's instruction (BORG Biotech, Zhengzhou). The absorption values of the reaction mixtures were measured at 450 nm. Each sample was analyzed with three biological replicates. The contents of GA isoforms in stem internodes of *TaGA2ox8-B1-2* overexpression (*TaGA2ox8-B1-2*-OE) lines and Fielder were determined following the procedures described in a previous study [17]. Three biological replicates were used for each sample.

*Quantitative PCR (qPCR) and RNA sequencing (RNA-seq) assays*

The stem internodes (Feekes 7.0) and developing grains (Feekes 10.5.4) of Fielder and the *TaGA2ox8-B1-2*-OE3 transgenic line were harvested and promptly frozen in liquid nitrogen. RNA extraction was performed using an RNA-prep Pure Plant kit following manufacturer's recommendations (Cat#DP441, Tiangen). Approximately 1 μg of RNA was used as template to synthesize first-strand cDNA with a PrimeScript RT Reagent kit (Cat#RR036B, Takara, Japan). qPCR was conducted with three biological replicates for each sample using 2 × Universal SYBR Green Fast qPCR Mix (Cat#RK21203, ABclonal, Wuhan) in a Bio-Rad CFX system (https://www.bio-rad.com/). The wheat *Actin* gene was used as an internal control. Relative expression of genes of interest calculated using the $2^{-\triangle\triangle CT}$ method [55].

Three biological replicates of the same stem internode samples were used for RNA-seq. RNA extraction, library construction and sequencing were carried out by Smart Genomics Company (https://smartgenomics.net/). A total of 10 Gb of sequencing data for each sample was obtained from the Illumina platform. Raw reads were first filtered through fastp with default parameters to get clean reads [56]. Clean reads were aligned to the IWGSC RefSeqv1.1 (https://plants.ensembl.org/Triticum_aestivum/Info/Index) [14] using HISAT2 v2.0.5 (https://daehwankimlab.github.io/hisat2) [57]. Reads were counted using FeatureCounts v1.5.0 [58] and the FPKM (fragments per kilobase million) value was calculated based on the length and the number of reads of each gene. Differential expression analysis was performed using the DESeq2 (1.16.1) R package (https://bioconductor.org/packages/release/bioc/html/DESeq2.html) [59]. Differentially expressed genes (DEGs) were defined by an adjusted $P$ value < 0.05 and $|\log_2(\text{fold change})| \geq 1$. GO (Gene Ontology) was used to define pathways involving the gene of interest using clusterProfiler 4.0. Normalized $\log_2$ (FPKM + 1) values of DEGs were shown on a heatmap using TBtools-II v2.152 [42].

*Network and phylogenetic analysis of haplotypes*

The wheat materials used for the analysis of haplotypic origin and spread were 306 landrace accessions with worldwide origin and 96 tetraploid accessions, and their variation information are available in VMap1.0 (https://ngdc.cncb.ac.cn/gvm/getProjectDetail?project=GVM000082) [60] and VMap2.0 (https://ngdc.cncb.ac.cn/gvm/getProjectDetail?project = GVM000720) [61]. One hundred and eight Chinese wheat cultivars released between 1920 and 2020 (Table S4) with re-sequencing information (https://www.ncbi.nlm.nih.gov/bioproject/PRJNA597250/) [25] were used to investigate changes in distribution of target haplotypes over time.

The haplotype network of target genes was constructed based on variation information for the above 306 landrace and 96 tetraploid accessions by popArt v1.7[62]. Phylogenetic analysis of haplotypes was achieved using the vcf2phylip v2.0 package (https://zenodo.org/records/2540861) with –r parameters.

*Statistical analysis*

Student's *t*-tests were performed to define the significance of differences in given traits between contrasting pairs of haplotypes in the natural population or between transgenic lines and Fielder (negative control). Multiple comparisons (Duncan's multiple range test, $P < 0.05$) were performed to analyze the significance among more than two haplotypes after running the Analysis Of Variance (ANOVA) using SAS v9.4 (https://support.sas.com/en/documentation/install-center/94/installation-guide-for-windows.html). Stable haplotype-trait associations for further analysis were those significantly detected in at least three environments and best linear unbiased estimation (BLUE) value.

## Results

*Genome-wide identification and phylogenetic analysis of TaGA2oxs*

The *TaGA2oxs* were described in a previous study [63] using the genomic resources at that time. To identify *TaGA2ox*s in a newly released genome, a genome-wide search was performed in IWGSC RefSeq1.1 by blastp in EnsemblPlants version 56 (https://plants.ensembl.org/Triticum_aestivum/Tools/Blast) using 11 OsGA2ox members as queries (Table S1). Forty wheat GA2oxs with complete domains were retrieved and documented according to orthologous relationships with OsGA2oxs and chromosomal positions in the wheat genome (Figs. 1a and S1; Table S1). Phylogenetic analysis according to formulated subfamilies in rice [30] classified the TaGA2oxs into three subgroups, C19-clade I, C19-clade II and C20-clade, each having 19, 6 and 15 members, respectively. The expanded numbers of *TaGA2ox* members of in wheat (40) relative to their respective orthologs in rice (11), maize (14), barley (11) and *Brachypodium distachyon* (12), were attributed to genome polyploidy and duplication. Most *TaGA2ox* genes (*TaGA2ox1*, *TaGA2ox2*, *TaGA2ox3*, *TaGA2ox4*, *TaGA2ox6*, *TaGA2ox7*, *TaGA2ox9*, *TaGA2ox10*, *TaGA2ox11* and *TaGA2ox12*) are present as single copy in the wheat sub-genomes (A, B and D). No *TaGA2ox* gene with genome-specific distribution was detected. *TaGA2ox12-A1* was transferred from 4AL to the terminal end of 4AS caused by chromosome inversion events. We also found a chromosome translocation event where *TaGA2ox13-A1* (*Rht12/TaGA2oxA13*) was transferred from chromosome arm 4AL to arm 5AL. Notably, tandem duplication events generated 2, 3 and 2 members at *TaGA2ox8-A1*, *TaGA2ox8-B1* and *TaGA2ox8-D1*, respectively. *TaGA2ox13-B1* locus included two tandem-duplication members. Genome synteny revealed that the wheat orthologs of *OsGA2ox8* included seven members generated from two tandem duplication events: the first duplication occurred before formation of temperate grasses and the second in the wheat B subgenome progenitor (possibly *Aegilops speltoides*, the closest species to the wheat B subgenome) (Fig. 1b; Table S5) [64]. *TaGA2ox12* genes are unique GA2ox family members of Triticeae crops and thus should originate from some of their progenitors that are currently unknown (Fig. 1c). *TaGA2ox13* genes, another unique group of members in the wheat A and B subgenomes, were generated before the first polyploidization event, where spontaneous chromosome doubling of a hybrid of *T. urartu*

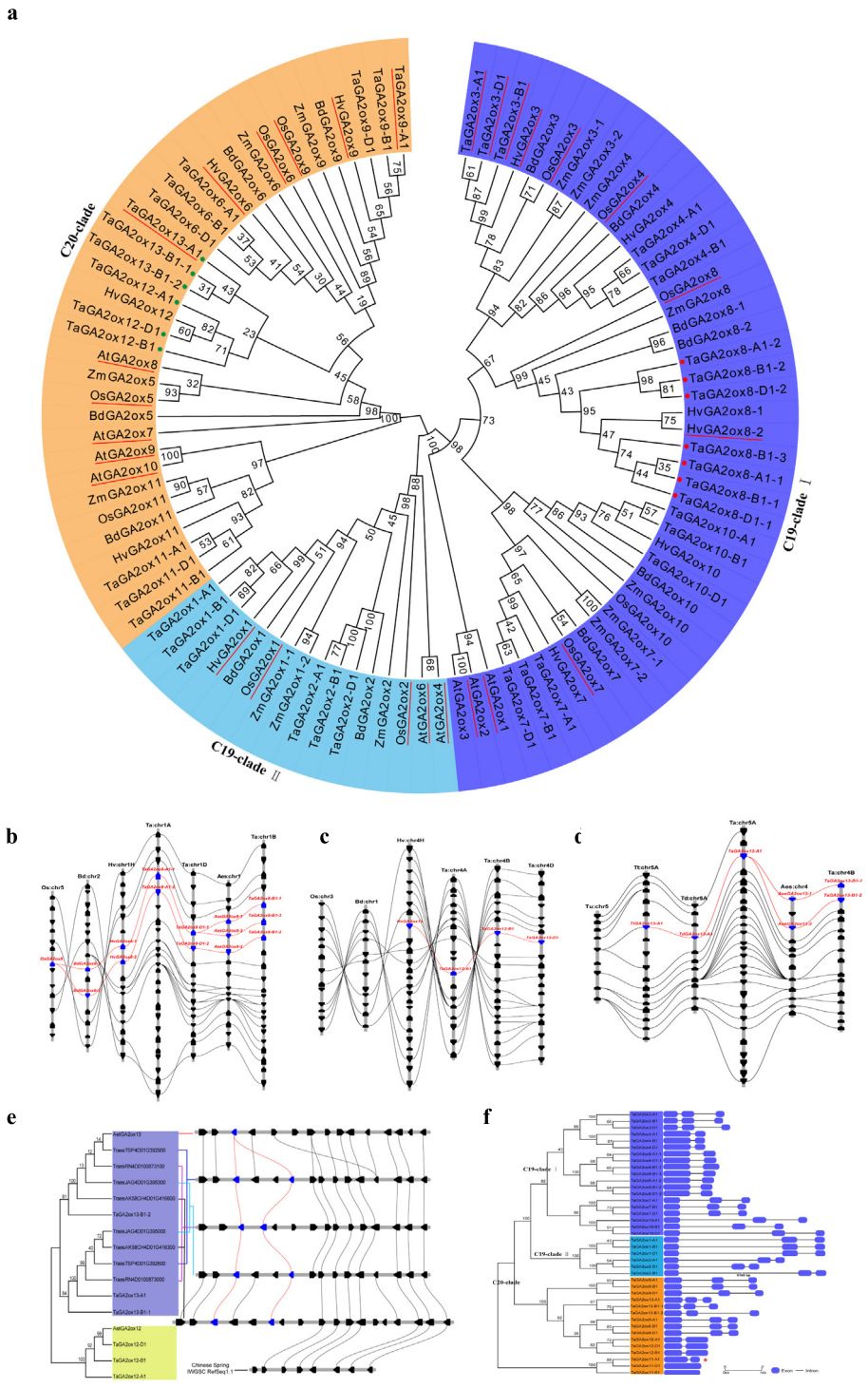


**Fig. 1. Genome-wide identification and characterization for wheat *gibberellin 2-oxidase* genes (*GA2oxs*)** (a) Phylogenetic tree of GA2ox homologs in six species. Information for GA2oxs from *Arabidopsis thaliana* (At), *Zea mays* (Zm), *Oryza sativa* (Os), *Brachypodium distachyon* (Bd), *Hordeum vulgare* (Hv), *Triticum aestivum* (Ta) is provided in Table S2. The GA2ox members in *Triticum aestivum* are named according to their chromosomal location and orthologous relationship with rice counterparts. Expansion of GA2oxs in *Triticum aestivum* are labeled with red or green dots. Functionally validated GA2oxs in different species are underlined. Three subfamilies of GA2oxs are highlighted in different colors. (b-d) Collinearity analyses of *TaGA2ox8* (b) *TaGA2ox12* (c) and *TaGA2ox13* (d) across some gramineous species including *Oryza sativa* (Os), *Brachypodium distachyon* (Bd), *Hordeum vulgare* (Hv), *Aegilops speltoides* (Aes), *Triticum turgidum* (Tt) and *Triticum durum* (Td), *Triticum urartu* (Tu), and *Aegilops tauschii* (Aet). Information for GA2ox8 homologs is provided in Table S5. (e) Identification of *TaGA2ox13* in D subgenomes across wheat cultivars and *Aegilops tauschii* (Aet) using phylogenetic tree (left) and synteny analysis (right). Homologous *GA2ox12* members are regarded as an outgroup. Information for *TaGA2ox13* homologs is listed in Table S5. (f) Gene structure analysis of 40 wheat *GA2oxs* based on phylogenetic relationships (left) and exon–intron patterns (right). The gene with annotation errors in the exon–intron pattern is labeled by the asterisk (*).

(AA) and the unknown B subgenome progenitor species (https://www.sciencedirect.com/topics/agricultural-and-biological-sciences/aegilops-speltoides) [65] gave rise to allotetraploid wild emmer (*T. turgidum* ssp. *dicoccoides*, AABB) (Fig. 1d). Additionally, a tandem duplication event formed two *TaGA2ox13* genes in the B subgenome, probably originated from *Aegilops speltoides*

(Fig. 1d; Table S5). However, *TaGA2ox13* is absent in the D subgenome, indicating that the gene might be lost from this subgenome during its evolution or was absent due to sequencing. To confirm our hypothesis, *TaGA2ox13-A1* (*Rht12*/*TaGA2oxA13*) was used as a query to search against the genome databases of *Aegilops tauschii*, the progenitor of wheat D subgenome. Indeed, a *TaGA2ox13* ortholog, temporarily named *AetGA2ox13*, was detected in *Aegilops tauschii*, (Table S5). We further performed homologous search against the de novo genome assembly of wheat cultivars using *AetGA2ox13* as a query. Some wheat cultivars, such as Aikang 58, Jagger and Renan, and *Triticum spelta* accession PI190962, have *TaGA2ox13* genes in chromosome 4D, indicating that the counterpart was absent in the IWGSC Chinese Spring reference genome (Fig. 1e; Table S5).

*TaGA2ox*s have diverse exon–intron structures with exon numbers ranging from one to three (Fig. 1f). *TaGA2ox11-B1* and *TaGA2ox11-D1* both have only one exon, but *TaGA2ox11-A1* has an intron according to the Chinese Spring RefSeq v1.1. We supposed that *TaGA2ox11-A1* should have no intron. We validated that *TaGA2ox11-A1* is intronless in Chinese Spring using reverse transcription PCR with the primers spanning the annotated intron, thus revealing an error in the annotation of this gene (Figs. S2a-c). The *TaGA2ox4*, *TaGA2ox8*, *TaGA2ox11* and *TaGA2ox12* genes each contained two exons, and the remaining *TaGA2ox*s had three (Fig. 1f). The *TaGA2ox12* and *TaGA2ox13* genes, located in homoeologous group 4 chromosomes and having the highest identity in protein sequence among *TaGA2ox* members, likely arose from segmental duplications. However, *TaGA2ox12* and *TaGA2ox13* have different exon–intron patterns, suggesting their independent evolutionary relationship. Like *OsGA2ox2* and *ZmGA2ox2*, *TaGA2ox2-B1* contains a long first intron, providing more opportunity for rearrangement between exons or playing an important role in transcriptional regulation [11,66,67]. We further performed a comprehensive collinearity analysis for *GA2ox* to identify the orthologous genes across different species (Table S6). We also conducted the genome-wide identification of *TaGA2ox*s in the pangenomes of wheat and found that there are copy number variations (CNVs) at *TaGA2ox8-B1*, *TaGA2ox8-D1* and *TaGA2ox13-D1* loci (Table S7).

### *Functional implication of TaGA2oxs based on function-validated orthologs, spatio-temporal expression patterns and genetic meta-analysis*

Two *TaGA2ox* members in wheat, *TaGA2ox9-A1* (*Rht24*/*TaGA2oxA9*) and *TaGA2ox13-A1* (*Rht12*/*TaGA2oxA13*), have been identified as causal genes for control of plant height [16,17]. Both *Rht12* and *Rht24* belong to the C20-clade, suggesting that the subfamily is important for wheat plant morphogenesis (Fig. 1a; Table S8). The functions of most *GA2ox* genes in Arabidopsis are well-defined [68–73]. Likewise, rice *GA2ox* genes are functionally validated, except for *OsGA2ox10* and *OsGA2ox11* [13,74–84]. A few *GA2ox* genes (*HvGA2ox1*, *HvGA2ox3*, *HvGA2ox6*, *HvGA2ox8-2* and *HvGA2ox9*) in barley, a wheat relative, were verified to modulate GA homeostasis and agronomic traits [85,86]. The summary of *GA2ox* gene information in model plants and crops in Table S8, provides clues regarding functional roles of wheat orthologs.

Since spatio-temporal expression provides fundamental information for understanding gene function in plant growth and development, we performed the *in silico* expression analysis of *TaGA2ox*s. Transcriptome datasets of Chinese Spring with high-quality de novo reference genome assembly were used to profile the expression patterns of *TaGA2ox*s in five tissues, including roots, stems, leaves, spikes and grains at three developmental stages (https://202.194.139.32/expression/wheat.html) [40]. The majority of *TaGA2ox*s exhibited high expression levels in at least one tested tissue, but had diverse spatio-temporal expression patterns. *TaGA2ox3*, *TaGA2ox4*, *TaGA2ox7*, *TaGA2ox9* and *TaGA2ox10* genes were highly expressed in most tissues, indicating that they were widely involved in vegetative and reproductive development. *TaGA2ox6* had higher transcript abundance in developing spikes, whereas *TaGA2ox8* genes were highly expressed in both spikes and stems (Fig. 2a; Table S9). *TaGA2ox4-A1* had much higher transcript level in roots than the orthologous genes in B and D subgenomes. Likewise, compared to *TaGA2ox13-A1* (*Rht12*/*TaGA2oxA13*) and *TaGA2ox13-B1-1*, *TaGA2ox13-B1-2* showed higher expression activity in leaves during late stages. These results suggested that the *TaGA2ox*s function in modulating agronomic traits through specific spatio-temporal expression.

To further determine the potential functions of *TaGA2ox*s in modulating agronomic traits, we co-localized these genes with reported genetic loci for plant height (PH), thousand grain weight (TKW), kernel number per spike (KNS), spike number per $m^2$ (SN), and heading date (HD). Twenty-six *TaGA2ox*s overlapping with, or adjacent to (<10 Mb), loci for agronomic traits formed 21 clusters (named Cluster 1–21) according to physical locations in the IWGSC RefSeq 1.1 (Fig. 2b; Table S10) [14]. Notably, 18 *TaGA2oxs* in 14 clusters co-located with genetic loci for plant height (Fig. 2b; Table S10). In accordance with previous studies, *Rht12*, *Rht24* and their respective orthologs (Clusters 15–19) had good genomic synteny with QTL for PH (Fig. 2b) [17,18]. Nine *TaGA2ox*s (*TaGA2ox2-B1*, *TaGA2ox2-D1*, *TaGA2ox8-B1-1*, *TaGA2ox8-B1-2*, *TaGA2ox8-B1-3*, *TaGA2ox11-1D1*, *TaGA2ox13-A1*/*Rht12*/*TaGA2oxA13*, *TaGA2ox13-B1-1* and *TaGA2ox13-B1-2*) were tightly linked with loci for yield components. *TaGA2ox7-A1* and *TaGA2ox11-D1* were close to QTL for HD. Overall, the genetic *meta*-analysis indicated that *TaGA2ox* members had wide functional diversity and pleiotropic effects on agronomic traits.

### *Identification of favorable haplotypes of TaGA2oxs*

Genome resequencing databases of 117 Chinese modern cultivars and 20 introduced cultivars in Wheat-SnpHub (https://wheat.cau.edu.cn/Wheat_SnpHub_Portal/) were used to identify allelic variations of *TaGA2ox*s (Table S2). Polymorphic sequence sites in genomic regions from 1.5 kb upstream to 500 bp downstream of *TaGA2ox* open reading frames (ORFs) were retrieved and analyzed. Fifty-two haplotypes among 19 *TaGA2oxs* were identified (Table S11). Gene-specific markers were developed to discriminate contrasting haplotypes (Table S3). Considering that major haplotypes usually have been subjected to artificial selection or/and natural domestication pressure, and thus are potentially valuable for wheat breeding, we selected haplotypes with frequencies of more than 15 % in our natural population for further analysis. To evaluate the genetic effects of these haplotypes, we performed marker-trait association analysis for PH, HD, grain yield and yield component traits (Table S12) [29]. Only *TaGA2ox* haplotypes with significant effects on agronomic traits are described below, due to the complexity of allelic variations and genetic effects. Allelic variations and genetic effects of *Rht12* and *Rht24* identified in this study were consistent with the results reported previously [17,18], and not included herein. We totally identified eight new favorable *TaGA2ox* haplotypes at five loci. Seven favorable haplotypes (*TaGA2ox6-B1_hap1*, *TaGA2ox8-B1-1_hap1*, *TaGA2ox8-B1-2_hap1*, *TaGA2ox8-B1-3_hap1*, *TaGA2ox9-B1_hap1*, *TaGA2ox9-B1_hap2* and *TaGA2ox10-A1_hap3*) reduce plant height without yield penalty. *TaGA2ox8-A1-1_hap2* significantly enhances grain yield and has little effect on plant height.

### *TaGA2ox6-B1*

Two single nucleotide polymorphisms (SNPs) in exons and one SNP in the downstream region of *TaGA2ox6-B1* were detected and

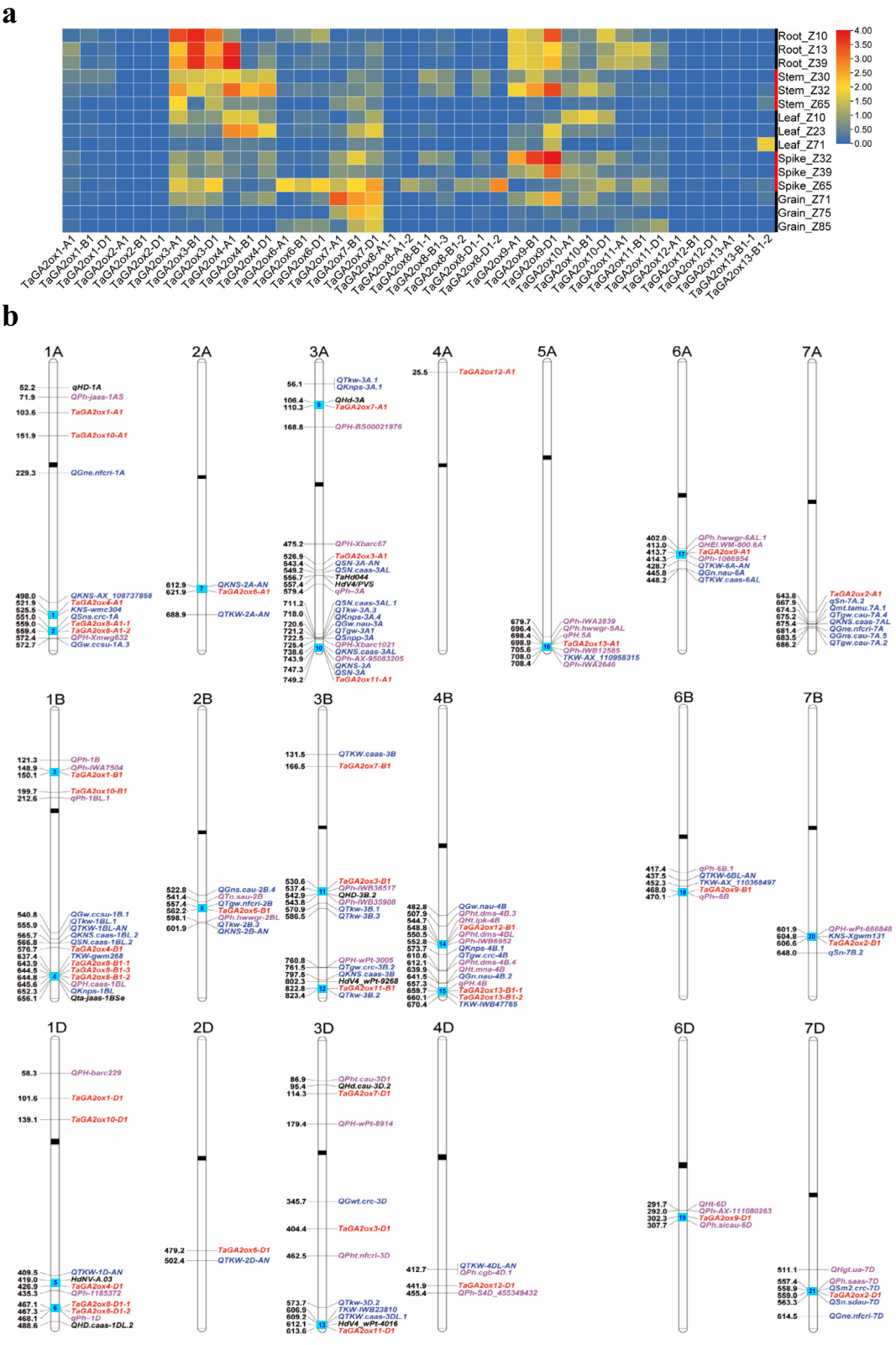


**Fig. 2. Spatio-temporal expression patterns (a) of wheat *gibberellin 2-oxidase* genes (*TaGA2oxs*) and their co-location (b) with genetic loci for agronomic traits (a)** Transcriptome dataset of Chinese Spring in the WheatOmics 1.0 database (http://202.194.139.32/expression/wheat.html) was used to profile expression patterns of *TaGA2ox* genes in five tissues (roots, stems, leaves, spikes, and grains) at three developmental stages; Z, Zadoks growth stages. **(b)** Numbers 1–21 in chromosomes are highlighted to indicate clusters of *TaGA2oxs* and loci for agronomic traits.

formed two haplotypes. A KASP marker 6-B1-KASP + 1276 developed according to an exonic SNP was used to genotype the natural population. *TaGA2ox6-B1_hap1* was associated with significantly reduced plant height compared to *TaGA2ox6-B1_hap2* (Fig. 3a; Table S12). Cultivars carrying *TaGA2ox6-B1_hap1* had higher grain yield and yield components than those with *TaGA2ox6-B1_hap2*,

albeit not significantly. These results indicated that *TaGA2ox6-B1_hap1* might be a favorable haplotype for wheat breeding.

*TaGA2ox8-A1-1*

One SNP detected in each of the upstream and downstream regions of *TaGA2ox8-A1-1* defined two haplotypes. A KASP marker 8-A1-1-KASP-104 was developed to genotype the natural population. *TaGA2ox8-A1-1_hap2* significantly decreased SN but enhanced the other two yield components TGW and KNS; notably, this haplotype empowered significantly increased grain yield (Fig. 3b; Table S12). Thus, *TaGA2ox8-A1-1_hap2* is a favorable haplotype. The high frequency of *TaGA2ox8-A1-1_hap2* (70.4 %) in the natural population suggested that this desirable haplotype had been subjected to positive selection.

*TaGA2ox9-B1*

One SNP and three insertion/deletion sites (InDels) in the upstream region, and two missense SNPs in the first exon of *TaGA2ox9-B1* were detected and defined four haplotypes (Fig. 3c). A GBTS marker 9-B1-GBTS-524–346-121 + 64 to diagnose the haplotypes simultaneously distinguished four polymorphic sites. The three major haplotypes (*TaGA2ox9-B1_hap1*, *TaGA2ox9-B1_hap2* and *TaGA2ox9-B1_hap3*) had frequencies of 21.7 %, 49.4 % and 21.2 %, respectively. Genetic effect analyses showed that *hap1* and *hap2* were associated with significantly reduced plant height compared to *hap3*. Cultivars carrying *hap1* or *hap2* have comparable grain yield as those with *hap3* (Fig. 3c; Table S12). Taken together, *TaGA2ox9-B1_hap1* and *TaGA2ox9-B1_hap2* are favorable alleles and were widely used in wheat breeding.

*TaGA2ox10-A1*

Three InDels and one SNP in the upstream region, one SNP in the first exon, and two SNPs in the downstream region of *TaGA2ox10-A1* formed five haplotypes *TaGA2ox10-A1_hap1-5* with the frequencies of 6.5 %, 3.2 %, 71.4 %, 1.3 % and 17.5 %, respectively, in the natural population. Among them, *TaGA2ox10-A1_hap3* and *TaGA2ox10-A1_hap5* were major haplotypes associated with significant differences in PH, KNS and SN. Cultivars carrying *TaGA2ox10-A1_hap3* had higher KNS but lower SN than those with *TaGA2ox10-A1_hap5*, suggesting that *TaGA2ox10-1A* modulates the trade-off between SN and KNS. Notably, *TaGA2ox10-A1_hap3* contributes to reduced plant height and enhanced yield potential compared to *TaGA2ox10-A1_hap5* (Fig. 3d; Table S12). Thus, *TaGA2ox10-A1_hap3* is a favorable allele and has been undergone artificial selection.

*Genetic dissection of tandem duplicated TaGA2ox8-B1 genes*

We previously identified QTL *QPH.caas.1BL* for PH at the end of chromosome arm 1BL in a Doumai × Shi 4185 recombinant inbred line (RIL) population [47]. It spanned three tandemly duplicated genes, *TaGA2ox8-B1-1 ~ 3*, according to gene annotation in IWGSC RefSeq 1.1 [14]. We identified the polymorphic sites spanning the *TaGA2ox8-B1* cluster based on the genome re-sequencing data of parents [87,88] and designed gene-specific markers (Table S13). Genetic mapping confirmed that the *TaGA2ox8-B1* genes were in the genetic region of *QPH.caas-1B*, suggesting they were the candidate genes in the QTL (Fig. 4a; Table S14). We further comprehensively detected their variations using resequencing databases in the wheat SnpHub (https://wheat.cau.edu.cn/Wheat_SnpHub_Portal/) [28]. Four SNPs in the exons and two SNPs in the downstream region of *TaGA2ox8-B1-1* were detected and defined four haplotypes. A GBTS marker 8-B1-1-GBTS + 1172 + 1244 + 1621 + 1637 designed to genotype the four SNPs in the second exon and downstream region distinguished the four haplotypes. Genotyping analysis showed that *TaGA2ox8-B1-1_hap2* was a rare allele with a frequency of 2.0 % in the natural population, whereas *hap1*, *hap3* and *hap4* had frequencies of 39.7 %, 30.8 % and 27.5 %, respectively (Fig. 4b). Six polymorphic sites in the ORF (1), upstream (3) and downstream (2) regions of *TaGA2ox8-B1-2*, defined four haplotypes. There was an InDel at –265 bp in the upstream region of *TaGA2ox8-B1-2* detected by genome resequencing data (Table S15). We developed an STS marker 8-B1-2-STS-265 to confirm the InDel. However, Sanger sequencing results showed that three alleles at the –265 site are detected with three types of inserts, CATGG, CGGGG or a 211-bp fragment, respectively (Fig. 4c). We also developed two GBTS markers 8-B1-2-GBTS-971 and 8-B1-2-GBTS + 1142 + 1410 + 1526 to diagnose the four haplotypes. Genotyping of the natural population showed that *TaGA2ox8-B1-2_hap1* and *TaGA2ox8-B1-2_hap2* were major haplotypes with frequencies of 35.3 % and 60.3 %, respectively. Only one SNP causing a missense mutation was identified in the first exon of *TaGA2ox8-B1-3*, and formed two haplotypes. Genotyping with GBTS marker 8-1B1-3-GBTS + 479 developed to identify the two haplotypes showed that *TaGA2ox8-B1-3_hap2* was a predominant haplotype with a frequency of 68.0 % in the natural population (Fig. 4d). Marker-trait association analysis displayed that *TaGA2ox8-B1-1_hap1*, *2_hap1* and *3_hap1* each was associated with significantly reduced PH and increased grain yield compared to the respective contrasting haplotype (Fig. 4b-d; Table S12). These favorable haplotypes were present in 31.9–––39.7 % of tested accessions, all lower than their contrasting haplotypes, suggesting they had not been subjected to positive selection and therefore have potential application in breeding. Linkage disequilibrium (LD) analysis in the natural population for genetic effects showed that the polymorphic sites in the *TaGA2ox8-B1* cluster define a strong haplotype block (Fig. S3a). We further conducted a combinational haplotype analysis for the gene cluster and defined twelve clustering haplotypes (*c_hap1-12*). Among them, three major haplotypes *c_hap1*, *c_hap7* and *c_hap10*, had distribution frequencies of 35.5 %, 27.4 % and 22.6 %, respectively (Fig. S3b). Genetic analysis showed that *c_hap1* was a favorable allele compared to other clustering haplotypes (Figs. S3c-h).

*Functional validation of TaGA2ox8-B1-2 as proof of concept*

Since three tandem duplicated *TaGA2ox8-B1* genes had consistent effects on multiple agronomic traits, we used *TaGA2ox8-B1-2* as a representative to validate their function and generated six independent transgenic overexpression (OE) lines. Three OE lines, OE3, OE5 and OE6 with relatively high expression levels of *TaGA2ox8-B1-2*, were chosen for subsequent analysis (Fig. 4e). Enzymatic activity of total GA2oxs in stems at jointing using enzyme linked immunosorbent assays (ELISA) confirmed that the OE lines had significantly higher GA2ox activity than Fielder, the negative control (Fig. 4f; Table S16). We further quantified GA isoforms in the internodes at the jointing stage and found that *TaGA2ox8-B1-2* had significant effect on the abundance of GA isoforms (Fig. 4g). Overexpression of *TaGA2ox8-B1-2* conferred significantly lower $GA_4$ but higher $GA_1$, suggesting that $GA_4$ is a key bioactive GA isoform in stem internodes (Fig. 4g). Although there are few biochemical studies on wheat GA metabolism, GA isoforms have been extensively analyzed in model plants and a regulatory network of GA metabolism and response was also proposed [75]. According the regulatory pathways of GA metabolism in model plants, we speculated that *TaGA2ox8-B1-2* modulated the conversion of bioactive $GA_4$ to inactive $GA_{34}$ based on the differential abundance of GA isoforms between the overexpression lines and Fielder (Fig. 4g). Phenotyping showed that the OE lines had a sig-

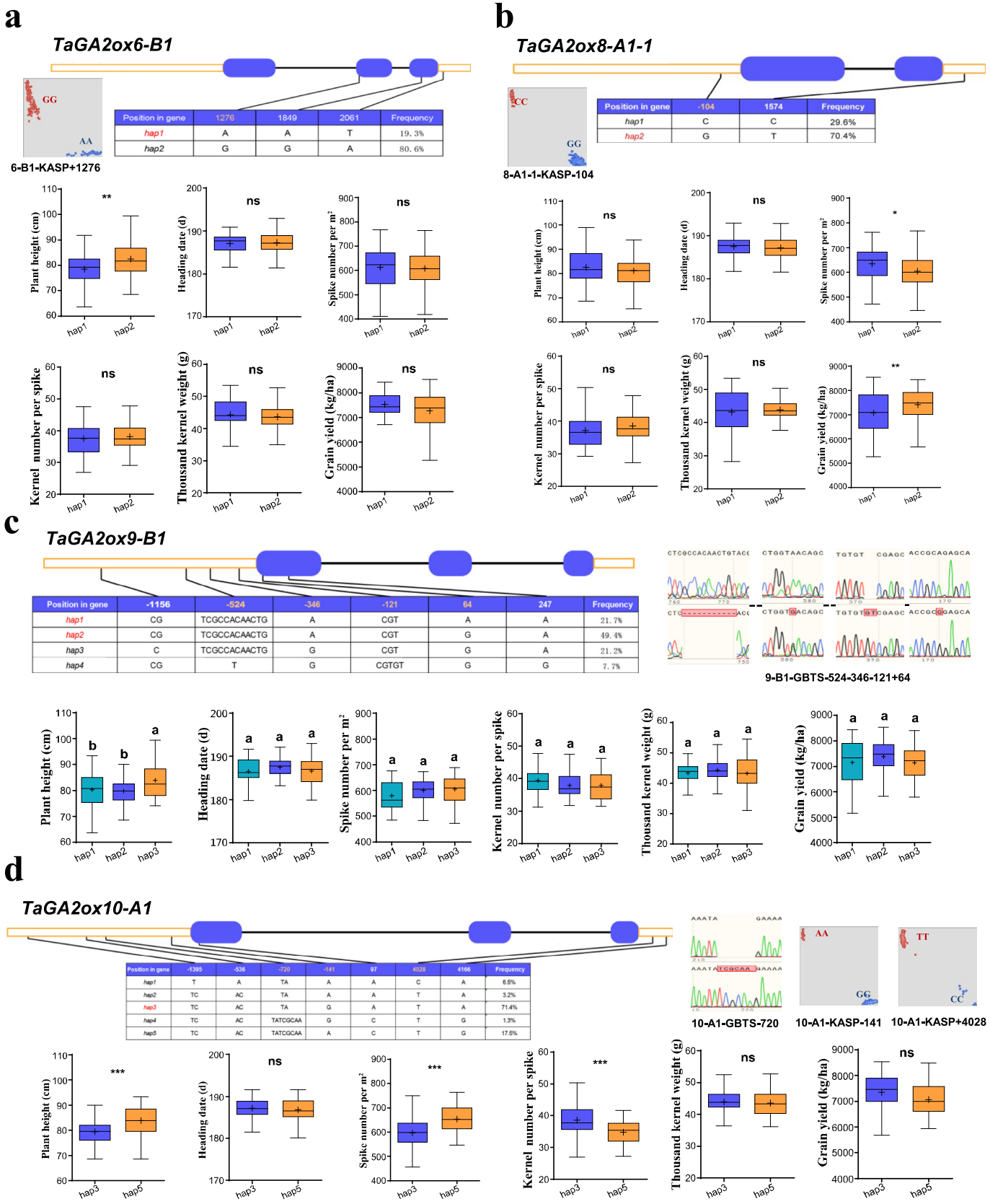


**Fig. 3. Genetic effects of major haplotypes of *TaGA2ox6-B1* (a), *TaGA2ox8-A1-1* (b), *TaGA2ox9-B1* (c) and *TaGA2ox10-A1* (d) on agronomic traits.** Blue boxes and solid lines indicate exons and introns, respectively, in the wheat *gibberellin 2-oxidase* genes (*TaGA2oxs*). In **(a-d)** for target *TaGA2oxs*, the 1.5 kb promoter and 500-bp downstream regions are shown by orange boxes (upper panel); kompetitive allele-specific PCR (KASP) or genotyping by targeted sequencing (GBTS) markers were developed to discriminate haplotypes and determine their frequency distribution in the natural population (middle panel); best linear unbiased estimation (BLUE) values for plant height, heading date, spike number per $m^2$, grain number per spike, thousand grain weight and grain yield of the panel population were used to define the genetic effects of these major haplotypes (lower panel). *, *** and ns, $P < 0.05$, $P < 0.001$, and not significant, respectively. For multiple comparisons, different letters on columns represent significant differences (Duncan's test, $P < 0.05$).

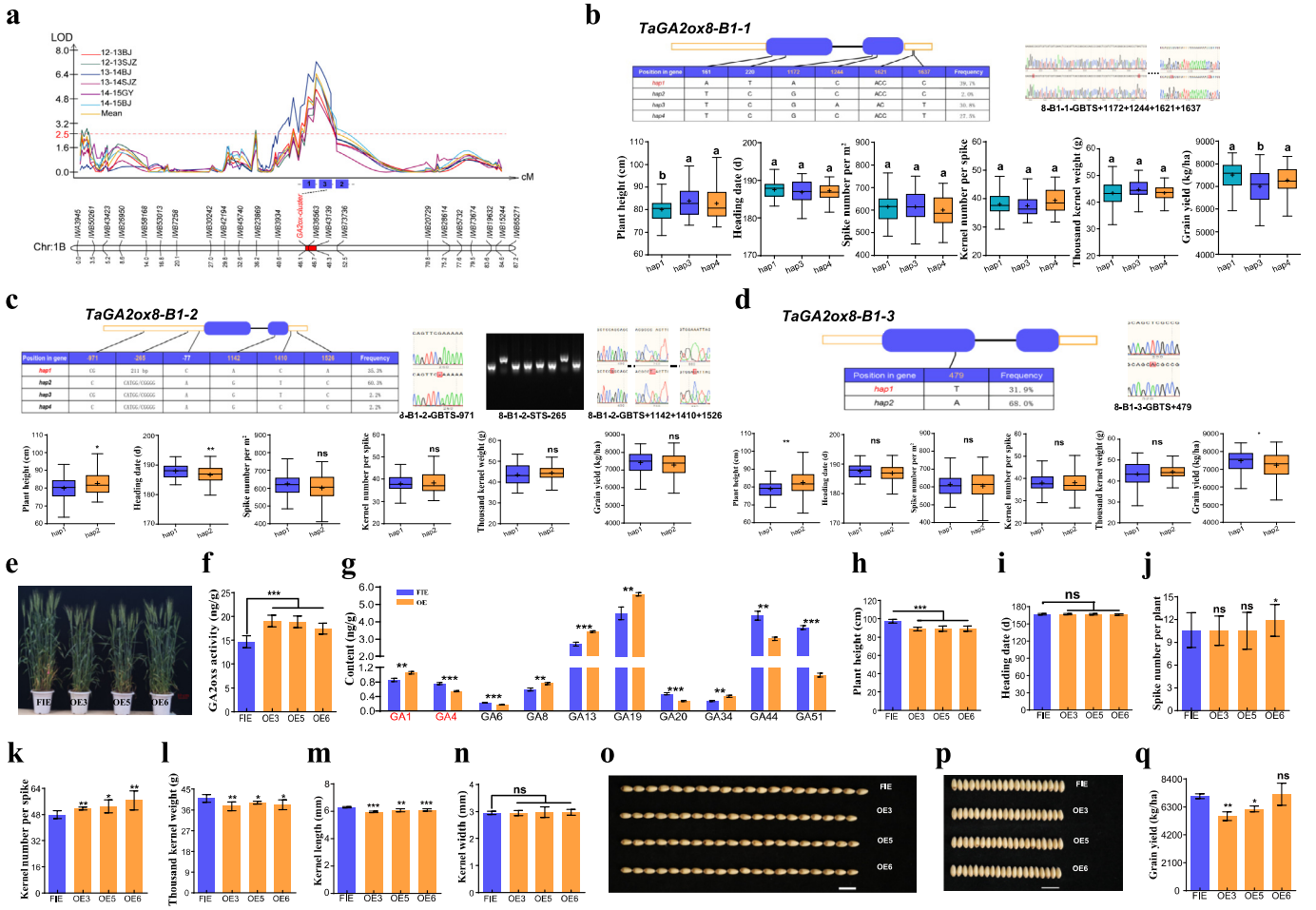


**Fig. 4. Genetic effects and functional dissection of the *TaGA2ox8-B1* cluster (a)** LOD contours of a QTL for plant height, spanning the *TaGA2ox8-B1* cluster. The horizontal and vertical axes indicate the LOD value and genetic markers, respectively. Contours in different colors indicate LOD contours of QTL for plant height on chromosome arm 1BL in different environments. BJ, Beijing; SJZ, Shijiazhuang; GY, Gaoyi; 12–13,13–14 and 14–15 represent 2012–2013, 2013–2014 and 2014–2015 cropping seasons, respectively. Genetic effects of a tandem-duplication *TaGA2ox8-B1-1* **(b)**, *TaGA2ox8-B1-2* **(c)** and *TaGA2ox8-B1-3* **(d)** on major agronomic traits in the natural population. In **(a-d)** for target genes, the 1.5-kb promoter and 0.5-kp downstream region are shown by orange boxes (upper panel); kompetitive allele-specific PCR (KASP), sequence-tagged site (STS) or genotyping by targeted sequencing (GBTS) markers were developed to discriminate different haplotypes and consequently determine their frequency distribution in the natural population (middle panel); best linear unbiased estimation (BLUE) values of plant height, heading date, spike number per $m^2$, grain number per spike, thousand grain weight and grain yield of the panel population were used to define the genetic effects of these major haplotypes (lower panel). For multiple comparisons, different letters on columns represent significant differences (Duncans test, $P < 0.05$). **(e)** Morphologic visualization of *TaGA2ox8-B1-2*-OE lines (OE3, OE5 and OE6) and Fielder (FIE). Bar, 10 cm. Statistical comparisons of enzymatic activity of total gibberellin 2-oxidases (GA2oxs) **(f)**, gibberellin (GA) isoform contents **(g)**, plant height **(h)**, heading date **(i)**, spike number per plant **(j)**, grain number per spike **(k)**, thousand kernel weight **(l)**, grain length **(m, o),** grain width **(n, p),** and grain yield **(q)** between *TaGA2ox8-B1-2*-OE lines and FIE.

nificant reduction (7.8–10.3 cm) in plant height compared to Fielder (Fig. 4h; Table S16). Moreover, the enhanced expression of *TaGA2ox8-B1-2* significantly increased KNS and reduced TKW, indicating this gene modulates trade-off between KNS and TKW (Fig. 4k and 4i; Table S16). *TaGA2ox8-B1-2* overexpression also significantly reduced grain length, suggesting that it affects grain weight largely by controlling grain size (Fig. 4m-p; Table S16). *TaGA2ox8-B1-2* has little function in regulating SN, as agreeing with its genetic effects of its natural variations, (Fig. 4j). Except for *TaGA2ox8-B1-2*-OE5, the other two OE lines had significantly decreased grain yield compared to Fielder, suggesting that overproduction of *TaGA2ox8-B1-2* had an adverse effect on grain yield (Fig. 4q; Table S16). To dissect the molecular mechanism of *TaGA2ox8-B1-2* in modulating plant height, we investigated DEGs in the stem internodes between the OE lines and Fielder at the jointing stage and detected 131 DEGs including 116 down-regulated and 15 up-regulated (Fig. S4a; Table S17). GO analysis indicated that many members of the bHLH, C2H2, ERF, MYB and WRKY transcription factor families were present among functional categories (Figs. S4b and S4c). Several DEGs were homologs of *EXPB11*, *WRKY50* and *WRKY28*, each of which were reported to regulate plant height (Table S17) [89–91]. *TaGA2ox8-B1-2* overexpression led to downregulation of homologs of *WRKY24* and *WRKY53*, suggesting that these genes mediated the function of *TaGA2ox8-B1-2* in repression of grain size (Table S17) [92,93]. qPCR confirmed that *WRKY24* (*TraesCS1A02G070400*, *TraesCS1B02G088900*, *TraesCS1D02G072900*, *TraesCS3A02G347500*, *TraesCS3B02G379200* and *TraesCS3D02G341100*), and *WRKY53* (*TraesCS1D02G418400*, *TraesCS5B02G183800* and *TraesCS5D02G190700*) were down-regulated in developing grains, and *WRKY28* (*TraesCS7A02G508800*) and *WRKY50* (*TraesCS1A02G358400*) were down-regulated in elongating stems (Fig. S4e). These results indicate that WRKY transcription factors are key downstream targets of *TaGA2ox8-B1-2*.

### *Evolutionary history and distribution for causal variations of TaGA2oxs*

The origin, spread trajectory and distribution of *TaGA2oxs* were traced to further determine their potency and prospects of the favorable haplotypes in wheat breeding. Considering that all favor-

able haplotypes of *TaGA2oxs* were identified in the A and B subgenomes, 96 tetraploid wheat accessions including the tetraploid progenitors of hexaploid wheat A and B subgenomes, and 306 hexaploid wheat landraces were selected to track origins. As landraces adapt to local environments and farming management systems, they can be viewed as evolving entities for studying migration and adaptation. By contrast, modern cultivars are usually developed in intensive breeding programs aimed at improving specific traits such as grain yield, disease resistance, and quality requirement. We therefore used landraces to investigate spread trajectory and geographic distribution of favorable haplotypes. We further investigated dynamic distribution of favorable haplotypes over different historical periods using a set of 108 Chinese landmark cultivars developed during the last century.

As already mentioned, the *TaGA2ox8-B1* cluster was tandemly duplicated. LD analysis in the 306 worldwide hexaploid and 96 tetraploid wheat accessions showed that polymorphic sites in the *TaGA2ox8-B1* cluster form a strong haplotype block (Fig. 5a). Twenty-one clustering haplotypes (*c_haps*) were defined, and among them five (*c_hap1*, *c_hap7*, *c_hap8*, *c_hap10*, *c_hap11*) were the same as those identified in genetic analysis (Table S18). The *c_hap1* was the desirable variation. The gene haplotype network revealed that this haplotype was detected only in hexaploid wheat, indicating that it evolved after hexaploidization (Fig. 5b). The *c_hap1* is a major variant in hexaploid wheat (Fig. 5c); its frequency increased from 44 % to 49 % during eastward expansion of landraces from West Asia (WA) to East Asia (EA). By contrast, the westward expansion to Europe resulted in a decrease to 26 % (Fig. 5d). Among Chinese landmark wheat cultivars, the *c_hap1* had a frequency of approximately 40 % during the 1920 s to 1960 s. Despite its frequent presence during that period, its frequency declined thereafter (Fig. 5e). The *c_hap7* and *c_hap10* with the frequencies of 31.0 % and 20.7 %, respectively, were the major undesirable haplotypes in the cultivars released during the last 20 years and thus should be subjected to selective sweep in favor of *c_hap1* in current breeding programs using gene-specific markers (Tables S3 and S19).

The haplotype network showed that the favorable haplotype *TaGA2ox6-B1_hap1* originated from wild emmer (Fig. S5a) and was a major haplotype in domesticated emmer and free-threshing tetraploids, demonstrating that it was subjected to artificial selection during domestication and cultural adaptation (Fig. S5b). *TaGA2ox6-B1_hap1* dispersal westward to Europe and eastward to EA resulted in similar proportions of 22 % and 21 %, respectively, comparable to that in WA (30 %), but it was eliminated during the eastward expansion from WA to Central and South Asia (CSA) (Fig. S5c). The proportion of *TaGA2ox6-B1_hap1* gradually increased from 7 % during the early stages of breeding in China (1920 s-1960 s) to 21 % during the last 20 years (2000 s to 2020 s) (Fig. S5d), suggesting it had undergone positive selection. Although the frequency of *TaGA2ox6-B1_hap2* gradually declined in Chinese landmark wheat cultivars over time, it was always the predominant haplotype (79–93 %).

*TaGA2ox8-A1* is the ortholog of *TaGA2ox8-B1* and comprises a gene cluster including *TaGA2ox8-A1-1* and *TaGA2ox8-A1-2*. Only *TaGA2ox8-A1-1_hap2* was identified as a favorable allele. Haplotype network showed that *TaGA2ox8-A1-1_hap2* was derived from a point mutation event of *TaGA2ox8-A1-1_hap3* and appeared in both wild domesticated emmer (Fig. S6a; Table S18). Although *TaGA2ox8-A1-1_hap2* was not detected in the tested free-threshing tetraploids, it was the predominant haplotype in wild and domesticated emmer (Fig. S6b). *TaGA2ox8-A1-1_hap2* disappeared during eastward expansion to CSA, but continued eastward dispersal increased its frequency to 14 %, equivalent to that in WA. Notably, *hap2* underwent a large increase (up to 50 %) in frequency during the westward spread to Europe and concomitantly became the predominant haplotype in Europe (Fig. S6c). Although *hap2* had a frequency of only 14 % in EA landraces, it was the predominant haplotype with a frequency of 67 % in Chinese landmark germplasms from 1920 s to 1960 s. This haplotype remained the predominant haplotype with frequencies of 67–86 % in Chinese cultivars during subsequent periods (Fig. S6d). Collectively, *TaGA2ox8-A1-1_hap2* has high frequency in wild emmer and is also widely present in both tetraploid and hexaploid wheat, suggesting that it has been subjected to selection during domestication and breeding worldwide.

*TaGA2ox9-B1* included two favorable haplotypes, *TaGA2ox9-B1_hap1* and *TaGA2ox9-B1_hap2*. The haplotype network showed that *hap2* was the major haplotype in both wild and domesticated tetraploid wheat, including wild, domesticated and free-threshing emmer, suggesting it was originated from wild emmer and was artificially selected during breeding of tetraploid wheat. By contrast, *hap1* was presumably derived from *hap2* since it was not present in wild emmer (Fig. S7a). Both *hap1* and *hap2* were major haplotypes in hexaploid wheat, indicating that they were positively selected (Fig. S7b). Although the proportion of two haplotypes decreased compared with that in WA during the westward range expansion to Europe, the dispersal eastward to EA enhanced the total proportion of *TaGA2ox9-B1_hap1* and *hap2* in CSA and EA landraces (Fig. S7c). The increasing percentage of *TaGA2ox9-B1_hap2* showed its renaissance in Chinese modern breeding programs, accompanying with a decreasing frequency of *TaGA2ox9-B1_hap1* (Fig. S7d).

Gene haplotype network indicated that the favorable haplotype *TaGA2ox10-A1_hap3* arose after the hexaploidization because it was only detected in hexaploid wheat (Figs. S8a-b). This haplotype has a stable frequency among wheat landraces during the expansion from WA to Europe, but was quite rare in the spread route from WA to CSA and EA. The frequency in the early Chinese cultivars is relatively high (40 %), suggesting that introduced European materials rather than Chinese landraces caused high frequency among Chinese landmark cultivars during 1920 s-1960 s (Fig. S8c). The proportion of *TaGA2ox10-A1-hap3* increased from the early stages of breeding (1920 s- 1960 s) to the last 20 years (2000 s to 2020 s) (Fig. S8d), and became the predominant haplotype with a frequency of 66 % in current Chinese wheat cultivars.

## Discussion

### *Favorable alleles of TaGA2oxs are important genetic resources for wheat improvement*

GA is essential for plant growth and development. Many genetic and functional analyses have proved that GA metabolic enzymes play an important role in regulating agronomic traits, especially plant height. GA2oxs catabolize bioactive GA inactivation or precursor GAs depletion [1]. *TaGA2ox9-A1* (*Rht24/TaGA2oxA9*) and *TaGA2ox13-A1* (*Rht12/TaGA2oxA13*) are the causal genes of *RHT24* and *RHT12*, respectively, and their favorable alleles have been widely used in wheat improvement [16–18]. The booming development of wheat genome sequencing programs and genotyping technologies facilitates identification of favorable variations of target genes. Here, we identified eight new favorable *TaGA2ox* alleles using genome resequencing data and genetic effect analysis. Several desirable haplotypes (*TaGA2ox6-B1_hap1*, *TaGA2ox8-B1-1_hap1*, *TaGA2ox8-B1-3_hap1*, *TaGA2ox8-B1-2_hap1*, *TaGA2ox9-B1_hap1*, *TaGA2ox9-B1_hap2* and *TaGA2ox10-A1_hap3*) reduce plant height without negative effects on yield. Additionally, three of them (*TaGA2ox8-A1-1_hap2*, *TaGA2ox8-B1-1_hap1* and *TaGA2ox8-B1-3_hap1*) significantly enhance grain yield. Genetic *meta*-analysis showed that these favorable genes were adjacent to the

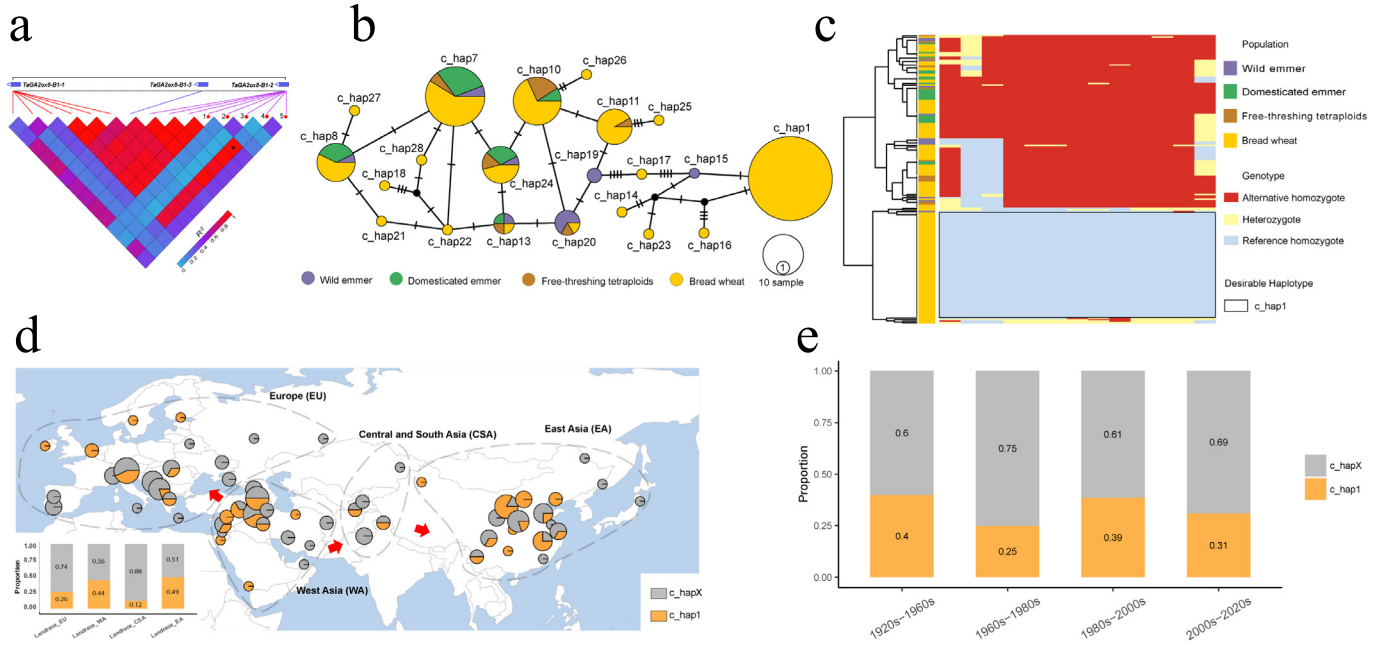


**Fig. 5. Phylogeny and selection of combined favorable haplotypes (*c_haps*) of the *TaGA2ox8-B1* gene cluster (a)** Linkage disequilibrium analysis of the *TaGA2ox8-B1* locus comprising tandemly duplicated genes *TaGA2ox8-B1-1* ~ *3* in the 306 worldwide bread wheat landraces and 96 tetraploid wheat accessions. Different colored lines represent different variants. Pairwise $R^2$ values for variation in each region are shown. The physical locations of the marked variations: 1: 644,799,104 bp, 2: 644,799,293 bp, 3: 644,799,503 bp, 4: 644,799,988 bp, and 5: 644,799,998 bp. **(b)** Haplotype network of *TaGA2ox8-B1* genes. 306 bread wheat landraces and 96 tetraploid wheat accessions were used to identify the *c_haps* of *TaGA2ox8-B1* and their evolutionary relationships. Each colored pie chart represents one unique haplotype and short lines between linked haplotypes indicate the number of mutations. Sequence variation of each haplotype is shown in Table S18. **(c)** The *c_hap* distribution of *TaGA2ox8-B1* in the tetraploid and bread wheat panels. Colored bars on the left represent different populations corresponding to (a). **(d)** Geographic distribution of the favorable *c_hap* of *TaGA2ox8-B1*. The 306 bread wheat landraces were used to trace the spread route of the favorable *c_hap*. The proportions of *TaGA2ox8-B1-c_hap1* (c_hap1) and the rest haplotypes (c_hapX) are shown in orange and gray, respectively. Landrace_EU and Landrace_WA, Landrace_EA, and Landrace_CSA represent landraces from Europe, West Asia, East Asia, and Central and South Asia, respectively. The map was constructed using the R package rworldmap. **(e)** Proportions of *c_hap1* and *c_hapX* in the Chinese landmark cultivars released during different historical periods.

previously identified genetic loci for plant height or/and yield component traits, suggesting that they are the causal genes for those loci and have stable effect in different genetic backgrounds. We further performed con-jointing analyses of these superior alleles to determine their combinatorial effects on plant height and grain yield as well as yield components. The cultivars with one, two, three, five and six favorable haplotypes harbor higher proportion (Fig. S9a). Wheat breeders have achieved plant height reduction without adverse effects on yield using reduced height (*Rht*) genes. As expected, more favorable haplotypes were associated with decreasing PH without yield penalty, demonstrating their cumulative effects on plant height (Figs. S9b-f). We also traced the origin, spread and global distribution of these dwarfing alleles to clarify their evolutionary history and application prospect. The majority of desirable *TaGA2ox* alleles were subjected to positive selection during artificial or/and natural domestication. These results strongly suggest that the eight favorable haplotypes have important application value for breeding. Therefore, *TaGA2ox*s are an important gene pool for wheat improvement, and their desirable alleles provide alternative genetic resources and molecular tools for plant height control.

Numerous rare *TaGA2ox* variants were detected in the natural population and some genes co-located with or were adjacent to genetic loci for agronomic traits (Fig. 2b and Table S11), but their genetic effects were not evaluated due to lack of statistical power. In near future, their genetic dissection should be performed using bi-parent mapping populations or additional natural populations, which may mine more new valuable alleles for wheat improvement. We also detected CNVs at *TaGA2ox8-B1* and *TaGA2ox8-D1* and *TaGA2ox13-D1* by gene synteny analyses across pan-genomes and found the CNVs ranging from one to five (Table S7). However, the phenotypes of those wheat accessions in same environments are not available. Thus, it is necessary to conduct long-read assemblies to study loci with duplicated genes. In future, we intend to identify genetic effects of the CNVs at *TaGA2oxs* based on genome long-read assemblies of a natural population.

The gain of function mutants in *TaGA2oxs* can cause appropriately reduced bioactive GAs and plant height, which is beneficial for wheat genetic improvement in breeding. As such, moderate upregulation of *TaGA2ox* expression is helpful to generate semi-dwarf wheat cultivars with high yield stability and potential because appropriately reduced plant height can enhance lodging resistance and harvest index. In fact. the gain of function variations in the promoter region conferred higher expression level of *TaGA2oxs* and moderate reduction in plant height [17,18].

### *Functional diversity of TaGA2oxs provide cues to dissect the mechanism underpinning plant morphogenesis and yield formation*

*TaGA2ox* genes harbor the common function of transforming bioactive GA isoforms into inactive ones. However, genetic effect analysis showed their diverse effects on agronomic traits. For *TaGA2ox2-B1,* there were five variations in the promoter, including three InDels and two SNPs and two exonic variations causing missense mutation (Table S11), but the potential functional variations had no obvious genetic effects in the tested materials (Table S11). Eight superior alleles had significant genetic effects on agronomic traits compared to their contrasting alleles. Seven of these alleles were associated with significantly reduced plant height, but they had different effects on grain yield. Among them, *TaGA2ox6-B1_hap1*, *TaGA2ox8-B1-2_hap1*, *TaGA2ox9-B1_hap1*, *TaGA2ox9-B1_hap2*, and *TaGA2ox10-A1_hap3* had little effect on grain yield,

whereas *TaGA2ox10-A1_hap3* significantly increased KNS and decreased SN, suggesting it is a regulator of trade-off between the two yield components. *TaGA2ox8-B1-1_hap1* and *TaGA2ox8-B1-3_hap1* significantly enhanced grain yield but had different effect on yield components. *TaGA2ox8-B1-1_hap1* improved grain yield by influencing KNS and SN, whereas *TaGA2ox8-B1-3_hap1* promoted grain yield by increasing SN.

*TaGA2ox8-B1-2* overexpression decreased the abundance of bioactive GA isoform $GA_4$, but increased the abundance of $GA_1$ in stem internodes. We previously determined the effect of *TaGA2ox9-A1* (*Rht24*/*TaGA2ox-A9*) on GA isoforms and found that its overexpression reduced the abundance of bioactive GA isoforms $GA_1$, $GA_4$ and $GA_7$ in stem internodes. Thus, *TaGA2ox* members maybe catalyze different substrates to maintain GA homeostasis. We compared DEGs in transcriptome analysis between *TaGA2ox8-B1-2*-OE and *TaGA2ox9-A1*-OE lines in equivalent spatio-temporal internodes and genetic backgrounds (common transgenic recipient Fielder) [17]. *TaGA2ox9-A1* overexpression caused drastically differential expression of 26,635 genes, whereas only 131 were differentially expressed between *TaGA2ox8-B1-2*-OE lines and Fielder. Although *TaGA2ox8-B1-2* and *TaGA2ox9-A1* caused the differential expression of 56 common genes, most of DEGs are unique in specific overexpression lines (Fig. S4d; Table S20), suggesting that *TaGA2ox* members control their own specific downstream genes to modulate agronomic traits. In all, *TaGA2ox* genes have diverse functions in regulating agronomic traits and the resultant genetic information facilitates broadening knowledge of mechanisms underlying GA-mediated plant morphogenesis, environmental adaptation and yield formation.

## Conclusion

Advent of genome sequencing and high-throughput genotyping technologies stimulated us to undertake a systemic characterization of *TaGA2ox* genes. Forty *TaGA2ox* genes were identified in wheat, and their expansion and function were specified. We retrieved major haplotypes of *TaGA2ox* genes and developed diagnostic markers. Eight new favorable haplotypes were associated with reduced plant height and without yield penalty were identified. Among them, tandemly duplicated *TaGA2ox8-B1-1_hap1*, *TaGA2ox8-B1-2_hap1* and *TaGA2ox8-B1-3_hap1* were validated as causal dwarfing allele of genetic locus *QPH.caas.1BL* for plant height. We further traced origin, spread and geographical distribution of the favorable haplotypes to clarify their evolution and implications for breeding. A large number of rare allelic variations were also identified and their breeding values remain to be determined in the specific populations. Overall, these findings provide a group of valuable gene resources and molecular tools for wheat breeding, and cues to uncover the genetic mechanism underlying gibberellin-mediated plant morphogenesis, yield formation and adaptation. An efficient pipeline that integrates population genomics, transgene assays and evolutionary analysis was also developed to identify gene family-scale favorable alleles and assess their application in wheat improvement.

## Declaration of competing interest

The authors declare that they have no known competing financial interests or personal relationships that could have appeared to influence the work reported in this paper.

## Acknowledgements

We are grateful to Prof. Robert McIntosh, Plant Breeding Institute, University of Sydney, for reviewing this manuscript. This work was supported by the National Key Research and Development Program of China (2022YFF1002904, 2022YFD1201500), the National Natural and Science Foundation of China (32472191), the Nanfan Special Project, CAAS (YBXM2303) and the Science and Technology Innovation Program of Chinese Academy of Agricultural Sciences (CAAS).

## Compliance with Ethics requirement

This article does not contain any studies with human or animal subjects.

## Appendix A. Supplementary data

Supplementary data to this article can be found online at https://doi.org/10.1016/j.jare.2025.08.025.

## References

[1] Binenbaum J, Weinstain R, Shani E. Gibberellin localization and transport in plants. Trends Plant Sci. 2018;23:410–21. doi: https://doi.org/10.1016/j.tplants.2018.02.005.
[2] Colebrook EH, Thomas SG, Phillips AL, et al. The role of gibberellin signaling in plant responses to abiotic stress. J. Exp. Biol. 2014;217:67–75. doi: https://doi.org/10.1242/jeb.089938.
[3] Davière JM, Achard P. A pivotal role of DELLAs in regulating multiple hormone signals. Mol. Plant 2016;9:10–20. doi: https://doi.org/10.1016/j.molp.2015.09.011.
[4] Xu H, Liu Q, Yao T, et al. Shedding light on integrative GA signaling. Curr. Opin. Plant Biol. 2014;21:89–95. doi: https://doi.org/10.1016/j.pbi.2014.06.010.
[5] Peng J, Richards DE, Hartley NM, et al. "Green revolution" genes encode mutant gibberellin response modulators. Nature 1999;400:256–61. doi: https://doi.org/10.1038/22307.
[6] Xu D, Bian Y, Luo X, et al. Dissecting pleiotropic functions of the wheat Green Revolution gene *Rht-B1b* in plant morphogenesis and yield formation. Development 2023;150:dev201601. doi: https://doi.org/10.1242/dev.201601.
[7] Hedden P, Phillips AL. Gibberellin metabolism: New insights revealed by the genes. Trends Plant Sci. 2000;5:523–30. doi: https://doi.org/10.1016/s1360-1385(00)01790-8.
[8] Monna L, Kitazawa N, Yoshino R, et al. Positional cloning of rice semidwarfing gene, *sd-1*: rice "Green Revolution gene" encodes a mutant enzyme involved in gibberellin synthesis. DNA Res. 2002;9:11–7. doi: https://doi.org/10.1093/dnares/9.1.11.
[9] Teng F, Zhai L, Liu R, et al. *ZmGA3ox2*, a candidate gene for a major QTL, *qPH3.1*, for plant height in maize. Plant J. 2013;73:405–16. doi: https://doi.org/10.1111/tpj.12038.
[10] Thomas SG, Phillips AL, Hedden P. Molecular cloning and functional expression of gibberellin 2-oxidases, multifunctional enzymes involved in gibberellin deactivation. Proceedings of the National Academy of Sciences, USA 1999;96:4698-4703. DOI: 10.1073/pnas.96.8.4698.
[11] Lo SF, Ho TD, Liu YL, et al. Ectopic expression of specific GA2 oxidase mutants promotes yield and stress tolerance in rice. Plant Biotechnol. J. 2017;15:850–64. doi: https://doi.org/10.1111/pbi.12681.
[12] Sakamoto T, Morinaka Y, Ishiyama K, et al. Genetic manipulation of gibberellin metabolism in transgenic rice. Nat. Biotechnol. 2003;21:909–13. doi: https://doi.org/10.1038/nbt847.
[13] Shan C, Mei Z, Duan J, et al. OsGA2ox5, a gibberellin metabolism enzyme, is involved in plant growth, the root gravity response and salt stress. PLoS One 2014;9:e87110. doi: https://doi.org/10.1371/journal.pone.0087110.
[14] Iwgsc. (International Wheat Genome Sequencing Consortium). Shifting the limits in wheat research and breeding using a fully annotated reference genome. Science 2018;361:eaar7191. doi: https://doi.org/10.1126/science.aar7191.
[15] Wang K, Shi L, Liang X, et al. The gene *TaWOX5* overcomes genotype dependency in wheat genetic transformation. Nat. Plants 2022;8(2):110–7. doi: https://doi.org/10.1038/s41477-021-01085-8.
[16] Buss W, Ford BA, Foo E, et al. Overgrowth mutants determine the causal role of gibberellin *GA2oxidaseA13* in *Rht12* dwarfism of wheat. J. Exp. Bot. 2020;71:7171–8. doi: https://doi.org/10.1093/jxb/eraa443.
[17] Tian X, Xia X, Xu D, et al. *Rht24b*, an ancient variation of *TaGA2oxA9*, reduces plant height without yield penalty in wheat. New Phytol. 2022;233:738–50. doi: https://doi.org/10.1111/nph.17808.
[18] Bian Y, Li L, Tian X, et al. *Rht12b*, a widely used ancient allele of *TaGA2oxA13*, reduces plant height and enhances yield potential in wheat. Theor. Appl. Genet. 2023;136:253. doi: https://doi.org/10.1007/s00122-023-04502-y.
[19] Guo W, Xin M, Wang Z, et al. Origin and adaptation to high altitude of Tibetan semi-wild wheat. Nat. Commun. 2020;11:508. doi: https://doi.org/10.1038/s41467-020-18738-5.

[20] Walkowiak S, Gao L, Monat C, et al. Multiple wheat genomes reveal global variation in modern breeding. Nature 2020;588:277–83. doi: https://doi.org/10.1038/s41586-020-2961-x.
[21] Sato K, Abe F, Mascher M, et al. Chromosome-scale genome assembly of the transformation-amenable common wheat cultivar "Fielder". DNA Res. 2021;28:dsab008. doi: https://doi.org/10.1093/dnares/dsab008.
[22] Shi X, Cui F, Han X, et al. Comparative genomic and transcriptomic analyses uncover the molecular basis of high nitrogen-use efficiency in the wheat cultivar Kenong 9204. Mol. Plant 2022;15:1440–56. doi: https://doi.org/10.1016/j.molp.2022.07.008.
[23] Jia J, Zhao G, Li D, et al. Genome resources for the elite bread wheat cultivar Aikang 58 and mining of elite homeologous haplotypes for accelerating wheat improvement. Mol. Plant 2023;16:1893–910. doi: https://doi.org/10.1016/j.molp.2023.10.015.
[24] Cheng H, Liu J, Wen J, et al. Frequent intra- and inter-species introgression shapes the landscape of genetic variation in bread wheat. Genome Biol. 2019;20:136. doi: https://doi.org/10.1186/s13059-019-1744-x.
[25] Hao C, Jiao C, Hou J, et al. Resequencing of 145 landmark cultivars reveals asymmetric sub-genome selection and strong founder genotype effects on wheat breeding in China. Mol. Plant 2020;13:1733–51. doi: https://doi.org/10.1016/j.molp.2020.09.001.
[26] Yang Z, Wang Z, Hu Z, et al. Comparative analysis of the genomic sequences between commercial wheat cultivars Jimai 22 and Liangxing 99. Acta Agron. Sin. 2020;46:1870–83. doi: https://doi.org/10.3724/SP.J.1006.2020.01009.
[27] Niu J, Ma S, Zheng S, et al. Whole-genome sequencing of diverse wheat accessions uncovers genetic changes during modern breeding in China and the United States. Plant Cell 2023;35:4199–216. doi: https://doi.org/10.1093/plcell/koad229.
[28] Wang W, Wang Z, Li X, et al. SnpHub: an easy-to-set-up web server framework for exploring large-scale genomic variation data in the post-genomic era with applications in wheat. GigaScience 2020;9.
[29] Li F, Wen W, Liu J, et al. Genetic architecture of grain yield in bread wheat based on genome-wide association studies. BMC Plant Biol. 2019;19:168. doi: https://doi.org/10.1186/s12870-019-1781-3.
[30] Zhang C, Nie X, Kong W, et al. Genome-wide identification and evolution analysis of the gibberellin oxidase gene family in six gramineae crops. Genes (Basel) 2022;13:863. doi: https://doi.org/10.3390/genes13050863.
[31] Li Y, Qin P, Sun A, et al. Genome-wide identification, new classification, expression analysis and screening of drought & heat resistance related candidates in the RING zinc finger gene family of bread wheat (*Triticum aestivum* L.). BMC Genomics 2022;23(1):696. doi: https://doi.org/10.1186/s12864-022-08905-x.
[32] Sun L, Song R, Wang Y, et al. New insights into the evolution of *CAF1* family and utilization of *TaCAF1Ia1* specificity to reveal the origin of the maternal progenitor for common wheat. J. Adv. Res. 2022;42:135–48. doi: https://doi.org/10.1016/j.jare.2022.04.003.
[33] Yang Y, Huang H, Xin Z, et al. Functional characterization of *TaWRKY254* in salt tolerance based on genome-wide analysis of the WRKY gene family in wheat core parent Zhou8425B. Plant Sci. 2025;357:112540. doi: https://doi.org/10.1016/j.plantsci.2025.112540.
[34] Voorrips RE. MapChart: Software for the graphical presentation of linkage maps and QTLs. J. Hered. 2002;93:77–8. doi: https://doi.org/10.1093/jhered/93.1.77.
[35] Kumar S, Stecher G, Tamura K. MEGA7: Molecular Evolutionary Genetics Analysis Version 7.0 for bigger datasets. Mol. Biol. Evol. 2016;33:1870–4. doi: https://doi.org/10.1093/molbev/msw054.
[36] Boden SA, McIntosh RA, Uauy C, et al. Updated guidelines for gene nomenclature in wheat. Theor. Appl. Genet. 2023;136(4):72. doi: https://doi.org/10.1007/s00122-023-04253-w.
[37] Chen Y, Song W, Xie X, et al. A collinearity-incorporating homology inference strategy for connecting emerging assemblies in the triticeae tribe as a pilot practice in the plant pangenomic era. Mol. Plant 2020;13:1694–708. doi: https://doi.org/10.1016/j.molp.2020.09.019.
[38] Rasko DA, Myers GS, Ravel J. Visualization of comparative genomic analyses by BLAST score ratio. BMC Bioinf. 2005;6:1–7. doi: https://doi.org/10.1186/1471-2105-6-2.
[39] Gu L, Li L, Wei H, et al. Identification of the group IIa *WRKY* subfamily and the functional analysis of *GhWRKY17* in upland cotton (*Gossypium hirsutum* L.). PLoS One 2018;13(1). doi: https://doi.org/10.1371/journal.pone.0191681.
[40] Ma S, Wang M, Wu J, et al. WheatOmics: a platform combining multiple omics data to accelerate functional genomics studies in wheat. Mol. Plant 2021;14:1965–8. doi: https://doi.org/10.1016/j.molp.2021.10.006.
[41] Zadoks JC, Chang TT, Konzak CF. A decimal code for the growth stage of cereals. Weed Res. 1974;14:415–21. doi: https://doi.org/10.1111/j.1365-3180.1974.tb01084.x.
[42] Chen C, Wu Y, Li J, et al. TBtools-II: a "one for all, all for one" bioinformatics platform for biological big-data mining. Mol. Plant 2023;16:1733–42. doi: https://doi.org/10.1016/j.molp.2023.09.010.
[43] Cao S, Xu D, Hanif M, et al. Genetic architecture underpinning yield component traits in wheat. Theor. Appl. Genet. 2020;133:1811–23. doi: https://doi.org/10.1007/s00122-020-03562-8.
[44] Xu D, Jia C, Lv X, et al. *In silico* curation of QTL-rich clusters and candidate gene identification for plant height of bread wheat. The Crop Journal 2023;11:1480–90. doi: https://doi.org/10.1016/j.cj.2023.05.007.
[45] Le GJ, Bordes J, Ravel C, et al. (2012) Genome-wide association analysis to identify chromosomal regions determining components of earliness in wheat. Theor. Appl. Genet. 2012;124:597–611. doi: https://doi.org/10.1007/s00122-011-1732-3.
[46] Wu X, Cheng K, Zhao R, et al. Quantitative trait loci responsible for sharp eyespot resistance in common wheat CI12633. Sci. Rep. 2017;7:11799. doi: https://doi.org/10.1038/s41598-017-12197-7.
[47] Li F, Wen W, He Z, et al. Genome-wide linkage mapping of yield-related traits in three chinese bread wheat populations using high-density SNP markers. Theor. Appl. Genet. 2018;131:1903–24. doi: https://doi.org/10.1007/s00122-018-3122-6.
[48] Chen Z, Cheng X, Chai L, et al. Pleiotropic QTL influencing spikelet number and heading date in common wheat (*Triticum aestivum* L.). Theor. Appl. Genet. 2020;133:1825–38. doi: https://doi.org/10.1007/s00122-020-03556-6.
[49] Hu J, Wang X, Zhang G, et al. QTL mapping for yield-related traits in wheat based on four RIL populations. Theor. Appl. Genet. 2020;133:917–33. doi: https://doi.org/10.1007/s00122-019-03515-w.
[50] Martinez AF, Lister C, Freeman S, et al. Resolving a QTL complex for height, heading, and grain yield on chromosome 3A in bread wheat. J. Exp. Bot. 2021;72:2965–78. doi: https://doi.org/10.1093/jxb/erab058.
[51] Benaouda S, Dadshani S, Koua P, et al. Identification of QTLs for wheat heading time across multiple-environments. Theor. Appl. Genet. 2022;135:2833–48. doi: https://doi.org/10.1093/jxb/erab058.
[52] Xie L, Liu S, Zhang Y, et al. Efficient proteome-wide identification of transcription factors targeting *Glu-1*: a case study for functional validation of TaB3-2A1 in wheat. Plant Biotechnol. J. 2023;21:1952–65. doi: https://doi.org/10.1111/pbi.14103.
[53] Ishida Y, Tsunashima M, Hiei Y, et al. Wheat (*Triticum aestivum* L.) transformation using immature embryos. Methods Mol. Biol. 2015;1223:189–98. doi: https://doi.org/10.1007/978-1-4939-1695-5_15.
[54] Hood EE, Gelvin SB, Melchers LS, et al. New *Agrobacterium* helper plasmids for gene transfer to plants. Transgenic Res. 1993;2(4):208–18. doi: https://doi.org/10.1007/BF01977351.
[55] Livak KJ, Schmittgen TD. Analysis of relative gene expression data using real-time quantitative PCR and the 2(-Delta Delta C(T)) method. Methods 2001;25:402–8. doi: https://doi.org/10.1006/meth.2001.1262.
[56] Chen S, Zhou Y, Chen Y, et al. Fastp: an ultra-fast all-in-one FASTQ preprocessor. Bioinformatics 2018;34:i884–90. doi: https://doi.org/10.1093/bioinformatics/bty560.
[57] Pertea M, Kim D, Pertea GM, et al. Transcript-level expression analysis of RNA-seq experiments with HISAT. StringTie and Ballgown Nature Protocols 2016;11(9):1650–67. doi: https://doi.org/10.1038/nprot.2016.095.
[58] Liao Y, Smyth GK, Shi W. FeatureCounts: an efficient general purpose program for assigning sequence reads to genomic features. Bioinformatics 2014;30(7):923–30. doi: https://doi.org/10.1093/bioinformatics/btt656.
[59] Love MI, Huber W, Anders S. Moderated estimation of fold change and dispersion for RNA-seq data with DESeq2. Genome Biol. 2014;15(12):550. doi: https://doi.org/10.1186/s13059-014-0550-8.
[60] Zhou Y, Zhao X, Li Y, et al. *Triticum* population sequencing provides insights into wheat adaptation. Nat. Genet. 2020;52:1412–22. doi: https://doi.org/10.1038/s41588-020-00722-w.
[61] Liu Y, Shen K, Yin C, et al. Genetic basis of geographical differentiation and breeding selection for wheat plant architecture traits. Genome Biol. 2023;24:114. doi: https://doi.org/10.1186/s13059-023-02932-x.
[62] Sheppard S, Méric G. Campylobacter ecology and evolution. Norfolk: Caister Academic Press ISBN:978-1-908230-36-2.
[63] Pearce S, Huttly AK, Prosser IM, et al. Heterologous expression and transcript analysis of gibberellin biosynthetic genes of grasses reveals novel functionality in the *GA3ox* family. BMC Plant Biol. 2015;15:130. doi: https://doi.org/10.1186/s12870-015-0520-7.
[64] Yang Y, Cui L, Lu Z, et al. Genome sequencing of Sitopsis species provides insights into their contribution to the B subgenome of bread wheat. Plant Commun. 2023;4:100567. doi: https://doi.org/10.1016/j.xplc.2023.100567.
[65] Ye F, Shen J, Zhao C, et al. Molecular characterization and evolutionary relationships of *avenin-like b* gene in *Aegilops speltoides*. J. Cereal Sci. 2023;109:103587. doi: https://doi.org/10.1016/j.jcs.2022.103587.
[66] Fu D, Szucs P, Yan L, et al. Large deletions within the first intron in *VRN-1* are associated with spring growth habit in barley and wheat. Mol. Genet. Genomics 2005;273:54–65. doi: https://doi.org/10.1007/s00438-004-1095-4.
[67] Li Y, Shan X, Jiang Z, et al. Genome-wide identification and expression analysis of the *GA2ox* gene family in maize (*Zea mays* L.) under various abiotic stress conditions. Plant Physiol. Biochem. 2021;166:621–33. doi: https://doi.org/10.1016/j.plaphy.2021.06.043.
[68] Schomburg FM, Bizzell CM, Lee DJ, et al. Overexpression of a novel class of gibberellin 2-oxidases decreases gibberellin levels and creates dwarf plants. Plant Cell 2003;15:151–63. doi: https://doi.org/10.1105/tpc.005975.
[69] Yamauchi Y, Takeda-Kamiya N, Hanada A, et al. Contribution of gibberellin deactivation by AtGA2ox2 to the suppression of germination of dark-imbibed *Arabidopsis thaliana* seeds. Plant Cell Physiol. 2007;48:555–61. doi: https://doi.org/10.1093/pcp/pcm023.
[70] Zhou B, Peng D, Lin J, et al. Heterologous expression of a gibberellin 2-oxidase gene from *Arabidopsis thaliana* enhanced the photosynthesis capacity in *Brassica napus* L. Journal of Plant Biology 2011;54:23–32. doi: https://doi.org/10.1007/s12374-010-9139-2.
[71] Lee D, Lee I, Kim K, et al. Expression of *gibberellin 2-oxidase 4* from Arabidopsis under the control of a senescence-associated promoter results in a dominant semi-dwarf plant with normal flowering. Journal of Plant Biology 2014;57:106–16. doi: https://doi.org/10.1007/s12374-013-0528-1.

[72] Wiesen LB, Bender RL, Paradis T, et al. A role for gibberellin 2-oxidase 6 and gibberellins in regulating nectar production. Mol. Plant 2016;9:753–6. doi: https://doi.org/10.1016/j.molp.2015.12.019.
[73] Chen Z, Liu Y, Yin Y, et al. Expression of AtGA2ox1 enhances drought tolerance in maize. Plant Growth Regul. 2019;89:203–15. doi: https://doi.org/10.1007/s10725-019-00526-x.
[74] Sakamoto T, Kobayashi M, Itoh H, et al. Expression of a gibberellin 2-oxidase gene around the shoot apex is related to phase transition in rice. Plant Physiol. 2001;125:1508–16. doi: https://doi.org/10.1104/pp.125.3.1508.
[75] Sakai M, Sakamoto T, Saito T, et al. Expression of novel rice gibberellin 2-oxidase gene is under homeostatic regulation by biologically active gibberellins. J. Plant Res. 2003;116:161–4. doi: https://doi.org/10.1007/s10265-003-0080-z.
[76] Lo SF, Yang SY, Chen KT, et al. A novel class of gibberellin 2-oxidases control semidwarfism, tillering, and root development in rice. Plant Cell 2008;20:2603–18. doi: https://doi.org/10.1105/tpc.108.060913.
[77] Huang J, Tang D, Shen Y, et al. Activation of gibberellin 2-oxidase 6 decreases active gibberellin levels and creates a dominant semi-dwarf phenotype in rice (*Oryza sativa* L.). J. Genet. Genomics 2010;37:23–36. doi: https://doi.org/10.1016/S1673-8527(09)60022-9.
[78] Liu C, Zheng S, Gui J, et al. *Shortened basal internodes* encodes a gibberellin 2-oxidase and contributes to lodging resistance in rice. Mol. Plant 2018;11:288–99. doi: https://doi.org/10.1016/j.molp.2017.12.004.
[79] Chen X, Tian X, Xue L, et al. CRISPR-Based assessment of gene specialization in the gibberellin metabolic pathway in rice. Plant Physiol. 2019;180:2091–105. doi: https://doi.org/10.1104/pp.19.00328.
[80] Hsieh KT, Liu SH, Wang IW, et al. *Phalaenopsis* orchid miniaturization by overexpression of *OsGA2ox6*, a rice GA2-oxidase gene. Bot. Stud. 2020;61:10. doi: https://doi.org/10.1186/s40529-020-00288-0.
[81] Hsieh K, Chen Y, Hu T, et al. Comparisons within the rice GA 2-oxidase gene family revealed three dominant paralogs and a functional attenuated gene that led to the identification of four amino acid variants associated with GA deactivation capability. Rice 2021;14:70. doi: https://doi.org/10.1186/s12284-021-00499-4.
[82] Li Z, Wang B, Zhang Z, et al. OsGRF6 interacts with SLR1 to regulate *OsGA2ox1* expression for coordinating chilling tolerance and growth in rice. J. Plant Physiol. 2021;260:153406. doi: https://doi.org/10.1016/j.jplph.2021.153406.
[83] Wang Y, Du F, Wang J, et al. Molecular dissection of the gene *OsGA2ox8* conferring osmotic stress tolerance in rice. Int. J. Mol. Sci. 2021;22:9107. doi: https://doi.org/10.3390/ijms22179107.
[84] Xing MQ, Chen SH, Zhang XF, et al. Rice OsGA2ox9 regulates seed GA metabolism and dormancy. Plant Biotechnol. J. 2023;21:2411–3. doi: https://doi.org/10.1111/pbi.14067.
[85] Ouellette L, Anh TP, Toora PK, et al. Heterologous functional analysis and expression patterns of gibberellin 2-oxidase genes of barley (*Hordeum vulgare* L.). Gene 2023;861:147255. doi: https://doi.org/10.1016/j.gene.2023.147255.
[86] Cheng J, Jia Y, Hill C, et al. Diversity of *gibberellin 2-oxidase* genes in the barley genome offers opportunities for genetic improvement. J. Adv. Res. 2024;S2090–1232(23):00408. doi: https://doi.org/10.1016/j.jare.2023.12.021.
[87] Song J, Xu D, Dong Y, et al. Fine mapping and characterization of a major QTL for grain weight on wheat chromosome arm 5DL. Theor. Appl. Genet. 2022;135:3237–46. doi: https://doi.org/10.1007/s00122-022-04182-0.
[88] Li L, Xu D, Bian Y, et al. Fine mapping and characterization of a major QTL for plant height on chromosome 5A in wheat. Theor. Appl. Genet. 2023;136:167. doi: https://doi.org/10.1007/s00122-023-04416-9.
[89] Breen J, Li D, Dunn DS, et al. Wheat beta-expansin (EXPB11) genes: Identification of the expressed gene on chromosome 3BS carrying a pollen allergen domain. BMC Plant Biol. 2010;10:99. doi: https://doi.org/10.1186/1471-2229-10-99.
[90] Chen Y, Liu L, Feng Q, et al. *FvWRKY50* is an important gene that regulates both vegetative growth and reproductive growth in strawberry. Hortic. Res. 2023;10:uhad115. doi: https://doi.org/10.1093/hr/uhad115.
[91] Zhang Z, Chen L, Yu J. Maize WRKY28 interacts with the DELLA protein D8 to affect skotomorphogenesis and participates in the regulation of shade avoidance and plant architecture. J. Exp. Bot. 2023;74:3122–41. doi: https://doi.org/10.1093/jxb/erad094.
[92] Tian X, He M, Mei E, et al. WRKY53 integrates classic brassinosteroid signaling and the mitogen-activated protein kinase pathway to regulate rice architecture and seed size. Plant Cell 2021;33:2753–75. doi: https://doi.org/10.1093/plcell/koab137.
[93] Tang J, Mei E, He M, et al. Functions of *OsWRKY24*, *OsWRKY70* and *OsWRKY53* in regulating grain size in rice. Planta 2022;255:92. doi: https://doi.org/10.1007/s00425-022-03871-w.